

The green valley is a red herring: Galaxy Zoo reveals two evolutionary pathways towards quenching of star formation in early- and late-type galaxies[★]

Kevin Schawinski,^{1†} C. Megan Urry,^{2,3,4} Brooke D. Simmons,⁵ Lucy Fortson,⁶ Sugata Kaviraj,⁷ William C. Keel,⁸ Chris J. Lintott,^{5,9} Karen L. Masters,^{10,11} Robert C. Nichol,^{10,11} Marc Sarzi,⁷ Ramin Skibba,¹² Ezequiel Treister,¹³ Kyle W. Willett,⁶ O. Ivy Wong¹⁴ and Suhyoung K. Yi¹⁵

¹*Institute for Astronomy, Department of Physics, ETH Zurich, Wolfgang-Pauli-Strasse 27, CH-8093 Zurich, Switzerland*

²*Department of Physics, Yale University, PO Box 208120, New Haven, CT 06520-8120, USA*

³*Yale Center for Astronomy and Astrophysics, Yale University, PO Box 208121, New Haven, CT 06520, USA*

⁴*Department of Astronomy, Yale University, PO Box 208101, New Haven, CT 06520-8101, USA*

⁵*Oxford Astrophysics, Denys Wilkinson Building, Keble Road, Oxford OX1 3RH, UK*

⁶*School of Physics and Astronomy, University of Minnesota, Minneapolis, MN 55455, USA*

⁷*Centre for Astrophysics Research, University of Hertfordshire, Hatfield, Herts AL1 9AB, UK*

⁸*Department of Physics and Astronomy, University of Alabama, Box 870324, Tuscaloosa, AL 35487, USA*

⁹*Adler Planetarium, 1300 S. Lakeshore Drive, Chicago, IL 60605, USA*

¹⁰*Institute of Cosmology and Gravitation, University of Portsmouth, Dennis Sciama Building, Burnaby Road, Portsmouth, PO1 3FX, UK*

¹¹*South East Physics Network; SEPNet; www.sepnet.ac.uk*

¹²*Center for Astrophysics and Space Sciences, Department of Physics, University of California, 9500 Gilman Drive, San Diego, CA 92093, USA*

¹³*Universidad de Concepción, Departamento de Astronomía, Casilla 160-C, Concepción, Chile*

¹⁴*CSIRO Astronomy and Space Science, PO Box 76, Epping, NSW 1710, Australia*

¹⁵*Department of Astronomy and Yonsei University Observatory, Yonsei University, Seoul 120-749, Republic of Korea*

Accepted 2014 February 17. Received 2014 February 5; in original form 2013 July 25

ABSTRACT

We use SDSS+GALEX+Galaxy Zoo data to study the quenching of star formation in low-redshift galaxies. We show that the green valley between the blue cloud of star-forming galaxies and the red sequence of quiescent galaxies in the colour–mass diagram is not a single transitional state through which most blue galaxies evolve into red galaxies. Rather, an analysis that takes morphology into account makes clear that only a small population of blue early-type galaxies move rapidly across the green valley after the morphologies are transformed from disc to spheroid and star formation is quenched rapidly. In contrast, the majority of blue star-forming galaxies have significant discs, and they retain their late-type morphologies as their star formation rates decline very slowly. We summarize a range of observations that lead to these conclusions, including UV–optical colours and halo masses, which both show a striking dependence on morphological type. We interpret these results in terms of the evolution of cosmic gas supply and gas reservoirs. We conclude that late-type galaxies are consistent with a scenario where the cosmic supply of gas is shut off, perhaps at a critical halo mass, followed by a slow exhaustion of the remaining gas over several Gyr, driven by secular and/or environmental processes. In contrast, early-type galaxies require a scenario where the gas supply and gas reservoir are destroyed virtually instantaneously, with rapid quenching accompanied by a morphological transformation from disc to spheroid. This gas reservoir destruction could be the consequence of a major merger, which in most cases

[★] This publication has been made possible by the participation of more than 250 000 volunteers in the Galaxy Zoo project. Their contributions are individually acknowledged at <http://www.galaxyzoo.org/Volunteers.aspx>.

† E-mail: kevin.schawinski@phys.ethz.ch

transforms galaxies from disc to elliptical morphology, and mergers could play a role in inducing black hole accretion and possibly active galactic nuclei feedback.

Key words: galaxies: active – galaxies: elliptical and lenticular, cD – galaxies: evolution – galaxies: spiral.

1 INTRODUCTION

Ever since the discovery of the bimodality in galaxy colour in the galaxy colour–magnitude and colour–mass diagrams from large-scale surveys (Strateva et al. 2001; Baldry et al. 2004, 2006), the colour space between the two main populations – the *green valley* – has been viewed as the crossroads of galaxy evolution. The galaxies in the green valley were thought to represent the transition population between the blue cloud of star-forming galaxies and the red sequence of quenched, passively evolving galaxies (e.g. Bell et al. 2004; Faber et al. 2007; Martin et al. 2007; Schiminovich et al. 2007; Wyder et al. 2007; Mendez et al. 2011; Gonçalves et al. 2012). Roughly speaking, all galaxies were presumed to follow similar evolutionary tracks across the green valley, with a fairly rapid transition implied by the relative scarcity of galaxies in the green valley compared to the blue cloud or red sequence.

The intermediate galaxy colours of green valley galaxies have been interpreted as evidence for the recent quenching of star formation (Salim et al. 2007). The clustering of active galactic nuclei (AGN) host galaxies in the green valley further suggested a role for AGN feedback in particular (e.g. Nandra et al. 2007; Hasinger 2008; Silverman et al. 2008; Cimatti et al. 2013). Galaxies in the green valley have specific star formation rates (sSFR) lower than the ‘main sequence’ of star formation in galaxies, which is a tight correlation between galaxy stellar mass and star formation rate (SFR), presumably as a result of quenching (e.g. Brinchmann et al. 2004; Elbaz et al. 2007; Noeske et al. 2007; Salim et al. 2007; Peng et al. 2010; Elbaz et al. 2011; Lee et al. 2012; Leitner 2012). Most star-forming galaxies live on the main sequence, so tracing the populations leaving the main sequence – those with lower sSFRs – probes the quenching mechanism(s) and, as Peng et al. (2010) showed, there may be at least two very different quenching processes.

Ultraviolet light comes predominantly from newly formed massive stars, which makes UV observations an excellent probe of the current rate of star formation. In this paper, we use UV–optical colours from *Galaxy Evolution Explorer* (*GALEX*) photometry (see e.g. Martin et al. 2007) to investigate the rate at which galaxies are decreasing their sSFR (i.e. how rapidly they change colour), and whether this correlates with morphology. Essentially, we use galaxy colours as stellar population clocks, an approach first conceived and applied by Tinsley and collaborators (Tinsley 1968; Tinsley & Gunn 1976; Tinsley & Larson 1978).

We interpret the evolutionary tracks of discs in terms of the gas supply and how star formation depletes the gas reservoir (Schmidt 1959). Interestingly, what had appeared to be outliers from the general parent galaxy population – namely, blue early types (Schawinski et al. 2009a) and red late types (Masters et al. 2010b) – far from being curiosities, are instead a valuable clue to galaxy evolution.

Morphology has not previously been a major ingredient in interpretations of the colour–mass diagram. Now that reliable morphological classifications have been made possible by citizen scientists in the Galaxy Zoo project (Lintott et al. 2008, 2011), we are able to investigate the relation of galaxy morphology to colour and mass. We also consider galaxy content and environment, now that stan-

dardized information is available for large galaxy samples (e.g. Baldry et al. 2004; Yang et al. 2007; Peng et al. 2010).

The Galaxy Zoo data have already enabled many insights about the link between galaxy evolution and colour (Schawinski et al. 2009a; Masters et al. 2010b) and about the link between galaxy evolution and environment (e.g. Bamford et al. 2009; Skibba et al. 2009), mergers (Darg et al. 2010a, b; Kaviraj et al. 2012; Teng et al. 2012), unusual galaxy types (Cardamone et al. 2009; Lintott et al. 2009; Keel et al. 2012) and specific morphological features such as bars (e.g. Hoyle et al. 2011; Masters et al. 2011, 2012; Skibba et al. 2012; Cheung et al. 2013; Melvin et al. 2014). In this paper, Galaxy Zoo morphologies provide the key to understanding that early- and late-type galaxies, even those with similar green optical colours, follow distinct evolutionary trajectories involving fundamentally different quenching modes.

Throughout this paper, we use a standard Λ CDM Cosmology ($\Omega_m = 0.3$, $\Omega_\Lambda = 0.7$ and $H_0 = 70 \text{ km}^{-1} \text{ s}^{-1} \text{ Mpc}^{-1}$), consistent with observational measurements (Komatsu et al. 2011). All magnitudes are in the AB system.

2 DATA

2.1 Catalogue generation, SDSS and multiwavelength data

We briefly describe the data used in this paper. The galaxy sample is based on public photometric and spectroscopic data products from the Sloan Digital Sky Survey (SDSS) Data Release 7 (York et al. 2000; Abazajian et al. 2009). The initial sample selection and properties are described in Schawinski et al. (2010a) and this catalogue is available on the web.¹ The sample is limited in redshift to $0.02 < z < 0.05$ and limited in absolute luminosity to $M_{z, \text{Petro}} < -19.50 \text{ AB}$, in order to create an approximately mass-limited sample. We adopt K -corrections to $z = 0.0$ from the New York University Value-Added Galaxy Catalog (NYU-VAGC; Blanton et al. 2005; Blanton & Roweis 2007; Padmanabhan et al. 2008). The typical $u - r \rightarrow {}^{0.0}u - r$ K -correction is $\sim 0.05 \text{ mag}$, and omitting the correction does not change any results significantly. We also obtain near-IR magnitudes from 2MASS (Skrutskie et al. 2006) via the NYU-VAGC.

We obtain aperture- and extinction-corrected SFRs and stellar masses from the Max Planck Institut for Astrophysics – Johns Hopkins University (MPA JHU) catalogue (Kauffmann et al. 2003; Brinchmann et al. 2004), which are calculated from the SDSS spectra and broad-band photometry. The spectroscopic classifications, especially the AGN-classifications, derive from analysis with the Gas AND Absorption Line Fitting (*GANDALF*) code (Cappellari & Emsellem 2004; Sarzi et al. 2006). Ultraviolet photometry for 71 per cent of our sample comes from the *GALEX* (Martin et al. 2005), matched via the Virtual Observatory. Observed optical and ultraviolet fluxes are both corrected for dust reddening using estimates of internal extinction from the public² stellar continuum

¹ See <http://data.galaxyzoo.org/>

² See <http://gem.yonsei.ac.kr/~ks0h/wordpress/>

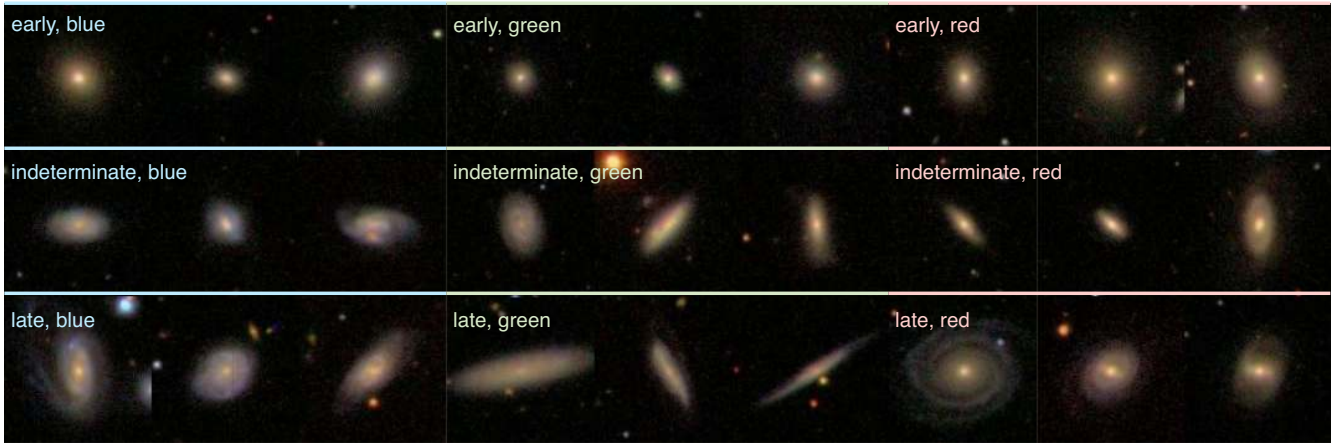


Figure 1. Example *gri* SDSS images ($51.2 \text{ arcsec} \times 51.2 \text{ arcsec}$), ordered by Galaxy Zoo classification. In the *top*, *middle* and *lower* rows are early-, indeterminate- and late-type galaxies, respectively. In each row, we show (from left to right) three blue-cloud, three green-valley and three red-sequence galaxies. The indeterminate-type galaxies are mostly composite bulge-disc systems that more closely resemble the late-type galaxies than the purely spheroidal early types. For this reason, it is not surprising that they mostly follow the late-type galaxies in their quenching behaviour.

fits performed by Oh, Sarzi, Schawinski & Yi (2011), applying the Cardelli, Clayton & Mathis (1989) law.

2.2 Galaxy Zoo visual morphology classifications

We use Galaxy Zoo 1 visual classifications of galaxy morphologies³ from the Galaxy Zoo citizen science project (Lintott et al. 2008, 2011). Using the CLEAN criterion developed by Land et al. (2008), which assigns a morphology to a galaxy when 80 per cent or more of Galaxy Zoo users agreed on the classification, we find that for our sample, 18 per cent are early types, 34 per cent are late types and 45 per cent are indeterminate types. The remaining 3 per cent are mergers.

Because we restrict our analysis to galaxies with clearly determined morphologies, it is important to understand what the (large) indeterminate category represents. Either these galaxies are composite bulge-disc systems in which neither the bulge nor disc clearly dominates, or the imaging data are not good enough for a clear classification. Inspection shows the former explanation likely accounts for the vast majority of the category, meaning we cannot classify these systems better even with deeper imaging. Fig. 1 shows example images of early-, indeterminate- and late-type galaxies. In terms of the Hubble tuning fork, the indeterminate types represent galaxies near the S0/Sa locus. For the most part, the indeterminate-morphology galaxies follow the trends of the late types, with only a small fraction being misclassified early types. We discuss this in more detail in Section 3.4.

Tables are cross-matched using the Virtual Observatory via Tool for OPERations on Catalogues And Tables (TOPCAT; Taylor 2005, 2011).

3 A JOURNEY THROUGH THE GREEN VALLEY: TWO EVOLUTIONARY PATHWAYS FOR QUENCHING STAR FORMATION

In this section, we look at how star formation varies in galaxies and consider variables that might affect star formation. We present

the well-known colour–mass diagram, first as it is observed for our galaxy sample (Section 3.1.1), then after correcting for dust reddening (Section 3.1.2). In both cases, sorting by morphology dramatically changes the impression of bimodality and thus drives a new interpretation of the green valley. We then present other observables relevant to characterizing galaxy evolution. UV constraints on current star formation (Section 3.3), environment density and halo mass (Section 3.5), atomic gas reservoir (Section 3.6) and black hole growth (Section 3.7).

Most star-forming galaxies exhibit a tight, nearly linear correlation (henceforth referred to simply as the ‘main sequence’) between galaxy stellar mass and SFR, which changes with redshift only in its normalization (at least out to $z \sim 2$, perhaps out to $z \sim 4$; Brinchmann et al. 2004; Elbaz et al. 2007; Noeske et al. 2007; Salim et al. 2007; Peng et al. 2010; Elbaz et al. 2011; Lee et al. 2012; Leitner 2012). This correlation between galaxy mass and SFR is likely the result of an equilibrium between galaxy inflows and outflows (see Bouché et al. 2010 and the ‘bathtub’ model of Lilly et al. 2013). Star-forming galaxies live on the main sequence regardless of whether they have spent a long time on it or have only recently re-started star formation. Accordingly, spending only a short time on the main sequence erases most of the past star formation history (in terms of galaxy colours). Then, when star formation is quenched, galaxies leave the main sequence, and we can interpret their changing colours as a reflection of the quenching process.

3.1 Galaxy colour bimodality as a function of morphology

We begin by showing that the green valley is not a single, unified population of galaxies, but rather a superposition of two populations that happen to exhibit the same intermediate (i.e. green) optical colours. The green valley is the space in the colour–mass diagram between the blue cloud and the red sequence; below we give a precise definition of the green valley in terms of $u - r$ colour. The interpretation of intermediate galaxy colours in terms of star formation histories is not original here; for example, it has been argued previously by Schawinski (2009), Cibinel et al. (2012) and Carollo et al. (2012).

³ Data publicly available at <http://data.galaxyzoo.org>.

3.1.1 The colour–mass diagram

The observed $u - r$ colour–mass diagrams of galaxies by morphology at $z \sim 0$ are shown in Fig. 2. Contours in each panel show the linear density of galaxies and green lines indicate the location of the green valley, defined from the all-galaxy panel at the upper left. The right-hand panels show only early types (top) or late types (bottom). These colour–mass diagrams, which constitute one of the two main starting points of our analysis, lead us to the following two important findings.

(i) Both early- and late-type galaxies span almost the entire $u - r$ colour range, that is, the classification by morphology reveals populations of blue early-type galaxies and of red late-type galaxies (e.g. Schawinski et al. 2009a; Masters et al. 2010b).

(ii) The green valley appears as a dip between bimodal colours only in the all-galaxies panel; within a given morphological class, there is no green valley, just a gradual decline in number density. Most early types lie in the red sequence with a long tail of ~ 10 per cent of the population reaching the blue cloud, which could represent a population in rapid transition, commensurate with the original idea of the green valley as a transition zone. The late-type galaxies, however, do not separate into a blue cloud and a red sequence, but rather form a continuous population ranging from blue to red without a gap or valley in between.

The traditional interpretation (and visual impression) from the all-galaxies diagram – that blue star-forming galaxies evolve smoothly

and quickly across the green valley to the red sequence – changes when viewed as a function of morphology.

Specifically, the impression of bimodality in the all-galaxies colour–mass diagram depends on the superposition of two separate populations: late types that are mostly in the blue cloud, decreasing smoothly all the way to the red sequence, and early types, a few of whose colours reach all the way to the blue cloud. Consideration of the indeterminate morphology galaxies (see Section 3.4) actually strengthens this conclusion, as they are mostly blue discs with prominent red bulges, hence the green colours.

The blue late-type galaxies, in particular, show no signs of rapid transition to the red sequence; indeed, they must take a very long time to reach the red sequence (Section 3.3). The early types do appear to transition quickly across the green valley, in that there are few of them with green colours and even fewer with blue colours. This suggests the bluest early types might have been produced by major mergers of late types.

The demographics of galaxies by colour and morphology in Table 1 make the point about evolutionary time-scale very clearly (for the moment ignoring changes from one morphology into the other): early types spend most of their time on the red sequence, while late types remain in the blue cloud for most of their lifetimes.

3.1.2 The extinction-corrected colour–mass diagram

Dust extinction reddens galaxies, and significant reddening from blue to red has been reported for high-redshift galaxies (e.g.

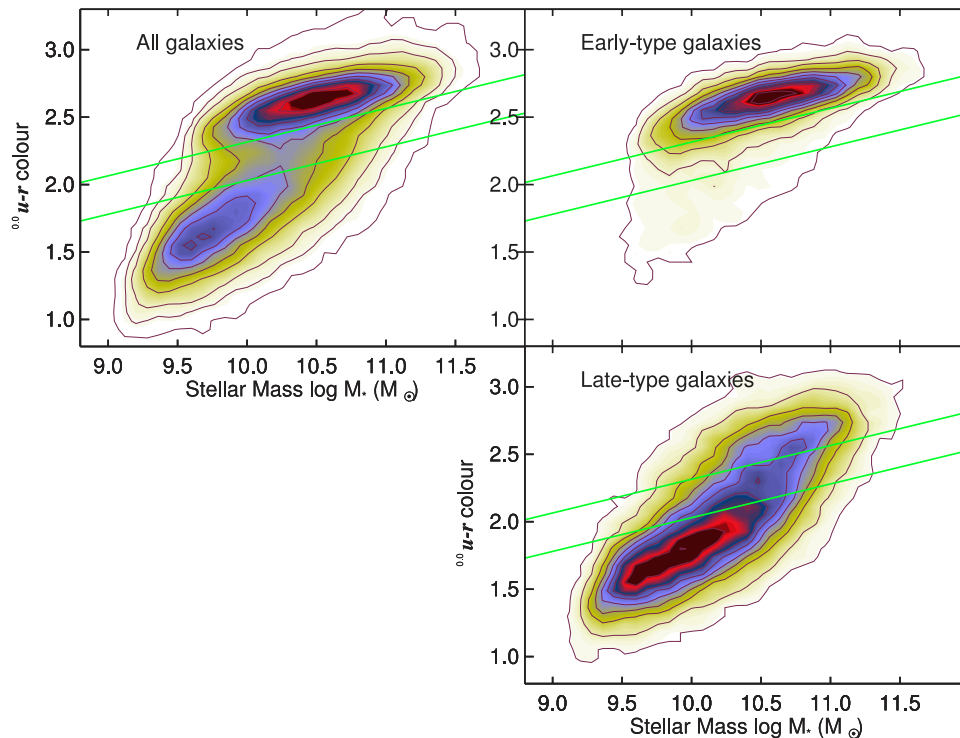
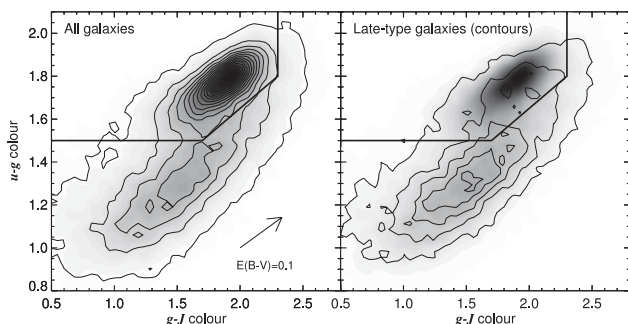


Figure 2. The $u - r$ colour–mass diagram for our sample. In the top left, we show all galaxies, whereas on the right, we show the early-type (top) and late-type galaxies (bottom); green lines show the green valley defined by the all-galaxy diagram. This figure illustrates two important findings: (1) Both early- and late-type galaxies span almost the entire $u - r$ colour range. Visible in the morphology-sorted plots are small numbers of blue early-type (top) and red late-type (bottom) galaxies (e.g. Schawinski et al. 2009a; Masters et al. 2010b). (2) The green valley is a well-defined location only in the all-galaxies panel (upper left). Most early-type galaxies occupy the red sequence, with a long tail (10 per cent by number) to the blue cloud at relatively low masses; this could represent blue galaxies transiting rapidly through the green valley to the red sequence. More strikingly, the late types form a single, unimodal distribution peaking in the blue (these are the main-sequence star formers) and reaching all the way to the red sequence, at higher masses, with no sign of a green valley (in the sense of a colour bimodality). The contours on this figure are linear and scaled to the highest value in each panel.

Table 1. Demographics of galaxies in the blue cloud, green valley and red sequence by morphology.

Galaxy sample	N	Per cent of population
Early-type, blue cloud	464	5.2 per cent
Early-type, green valley	1110	12.4 per cent
Early-type, red sequence	7404	82.5 per cent
<i>Early-type, all</i>	8978	100 per cent
Late-type, blue cloud	12 380	74.1 per cent
Late-type, green valley	3152	18.9 per cent
Late-type, red sequence	1175	7.0 per cent
<i>Late-type, all</i>	16 707	100 per cent

**Figure 3.** The ugJ colour–colour diagram for our sample, analogous to the UVJ diagram of Williams et al. (2009). The arrow indicates the shift due to dust for an $E(B-V) = 0.1$ using a Calzetti et al. (2000) extinction law. In the left-hand panel, we show all galaxies and an adapted box separating passive red galaxies from dusty star-forming galaxies. The right-hand panel shows the (same) shading of the entire galaxy sample, with contours for late-type galaxies only; this shows that some of the red spirals are actually dust-reddened spirals, while others are passively evolving.

Brammer et al. 2009; Williams et al. 2009; Cardamone et al. 2010), although this effect should be of limited importance at low redshift, where sSFR and gas fractions are lower. Nevertheless, since we are focusing on the quenching of star formation, we must first assess the effect of dust in moving intrinsically blue galaxies from the blue cloud to the green valley or the red sequence. In particular, significant amounts of dust in inclined spirals have been reported by Masters et al. (2010a), and Sodr , Ribeiro da Silva & Santos (2013) have shown that the reddest galaxies in the local Universe are edge-on discs.

We use the $U - V$ versus $V - J$ approach introduced by Williams et al. (2009) to separate dusty red galaxies from passive red galaxies. In Fig. 3, we show the very similar $u - g$ versus $g - J$ diagram (using SDSS+2MASS data), from which we conclude that there are some dusty, star-forming galaxies at low redshift (upper-right side of left-hand panel). Most of these are late-type galaxies (right-hand panel) and many are highly inclined spirals (as traced by the b/a axis ratio; see also Masters et al. 2010a). Muzzin et al. (2013) similarly found that the dusty starburst part of the $U - V$ versus $V - J$ diagram at low redshift contains some objects, but far fewer than at high redshift.

Even though the effect is small, we correct the $u - r$ colours using an estimate of the extinction in the stellar continuum. We take the measured $E(B-V)$ values from Oh et al. 2011 (based on the GANDALF code Cappellari & Emsellem 2004; Sarzi et al. 2006), and use the Calzetti et al. (2000) extinction law; for the GALEX magnitudes,

we use the Cardelli et al. (1989) law. We show this dust-corrected colour–mass diagram in Fig. 4.

The main differences after correcting for dust reddening are that the blue cloud (i.e. the main sequence) is now bluer, and the slope to redder colours with increasing mass flattens (presumably driven by dust from higher SFRs). The separation of the blue cloud and red sequence also becomes more prominent. Vivially, the green valley population in both the early- and late-type population does not disappear, and red late-type galaxies remain; not all of them were dusty starformers. Thus, dust correction is important but does not greatly change the global picture.

We now define the green valley population on the dust-corrected colour–mass diagram for all galaxies (upper-left panel of Fig. 4):

$$^{0.0}u - r(M_{\text{stellar}}) = -0.24 + 0.25 \times M_{\text{stellar}}, \quad (1)$$

$$^{0.0}u - r(M_{\text{stellar}}) = -0.75 + 0.25 \times M_{\text{stellar}}. \quad (2)$$

We refer to galaxies satisfying this colour criterion as green valley galaxies, even as we argue this term does not have a simple physical meaning. Table 1 presents general demographic information about the early- and late-type galaxies. These results are insensitive to adjustments of the specific boundaries of the green valley.

3.2 The different recent star formation histories of early- and late-type galaxies

We now consider *why* galaxies are in the green valley. The analysis in Section 3.1.2 shows that dust extinction is not the main reason. Instead, we show here that early- and late-type galaxies have very different recent star formation histories which result, coincidentally, in the same green valley colours.

3.2.1 Green valley galaxies are offset from the main sequence of star formation

Fig. 5 shows the stellar mass versus SFR (from aperture-corrected $H\alpha$) and sSFR diagrams, with the green valley early- and late-type galaxies highlighted. The grey contours show the main star-forming population (of all morphologies), identified spectroscopically, while the green valley objects are plotted regardless of emission line class. (This means that some fraction of the SFRs and sSFRs are upper limits.)

Fig. 5 shows that green valley galaxies (green points) are objects that have moved off the main sequence. That is, since virtually all star-forming galaxies are on the main sequence and since green valley galaxies must have experienced star formation in the past, something has moved them off the main sequence. The solid black line shows the local main sequence with a slope⁴ β of -0.2 (based on DR7 data; $\beta = -0.1$ for DR4; Y. Peng, private communication), with dashed lines indicating ± 0.3 dex. The grey dashed lines show further 0.3 dex offsets down from the main sequence. From both the SFR and sSFR diagrams, it is apparent that both early- and late-type galaxies in the green valley are also off the main sequence – as expected because they are in the process of quenching. What this diagram does not reveal is *how fast* galaxies are moving off the main sequence.

To complete the circle, we return to the colour–mass diagram and combine it with sSFR information. In Fig. 6, we show the

⁴ Where β is the exponent in $\text{sSFR} \propto M_{\text{stellar}}^{\beta}$.

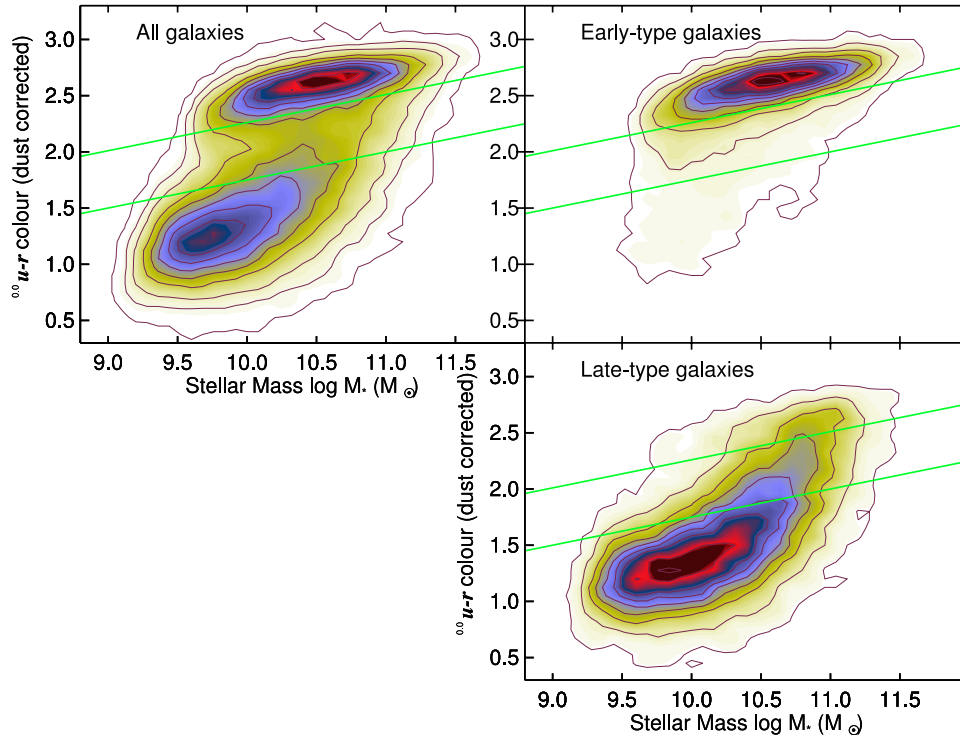


Figure 4. The reddening-corrected $u - r$ colour–mass diagram for our sample. Same as Fig. 2, but the $u - r$ colour is corrected by the $E(B - V)$ in the stellar continuum, as measured in the SDSS spectra using the GANDALF code (Oh et al. 2011). Compared to Fig. 2, there are no significant changes; in particular, very few green or red late-type galaxies actually belong in the blue cloud. The slope of the disc galaxy contours becomes more horizontal, making clear that late types evolve more slowly than early-type galaxies. Moreover, there is clearly a tail of galaxies rising above the blue cloud at high masses, whereas the blue tail of the early types is towards low masses. While some red late types are indeed dust-reddened, intrinsically blue galaxies, many are not, and the overall sense remains that the colours of late-type galaxies change slowly. The green valley defined here, from the all-galaxies panel (upper left), is used throughout the rest of this paper. The contours on this figure are linear and scaled to the highest value in each panel.

(dust-corrected) colour–mass diagram, analogous to Fig. 4 except that we colour 0.1×0.1 dex panels by the average sSFR in each bin. Not too surprisingly, this reveals a good correlation between dust-corrected $u - r$ colour and sSFR, showing that the green valley is, as expected, the region in colour–mass space where sSFRs have declined as galaxies have moved off the main sequence. Still, like the original colour–mass diagram, this figure does not reveal the time-scales on which the sSFRs decline, so in a sense it obscures the fact (presented below) that early- and late-type galaxies transition very differently through the green valley.

We note that the increasing prominence of bulges in massive, red late types (e.g. Masters et al. 2010b) does not significantly alter the $u - r$ colour for the present sample: Fig. 5 makes it clear that all intrinsically green galaxies (the green points) are off the main sequence regardless of morphology. Star-forming late types on the main sequence that would appear green in $u - r$ colour due to a luminous, red bulge have either been excluded (such objects are likely to be classified as ‘indeterminate’ since they have both bulge and disc) or, if classified as bona fide late types, the young blue stars simply outshine the red bulge.

3.3 UV–optical colour–colour diagrams constrain the star formation quenching time-scale

O- and B- and A-stars have very different colours and lifetimes and thus can provide leverage over the very recent star formation histories of galaxies. The SFR and sSFR diagrams, with SFRs based on $H\alpha$ line emission, provide a constraint on recent star formation

properties but not on how rapidly the (s)SFR is changing. $H\alpha$ traces the OB stars on time-scales of $10^6 - 10^7$ yr, the rest-frame UV traces the range of $10^7 - 10^8$ yr while optical colours are sensitive up to 10^9 yr. We use a UV–optical colour–colour diagram, which takes into account the age differential probed by the UV–optical of the spectral energy distribution (SED). This UV–optical colour–colour diagram thus is sensitive to the time derivative of the SFR, to argue that the current star formation histories of green valley early- and late-type galaxies are, in fact, very different.

Fig. 7 shows the (dust-corrected) $NUV - u$ versus $u - r$ colour–colour diagrams of local galaxies. In the top-left panel, we show the entire galaxy population (grey contours) and the green valley early- and late-type galaxies (orange and blue contours, respectively). In the top-right panel, we show only the early-type galaxies, and in the bottom-right panel, only the late-type galaxies, with the green valley populations again as orange and blue contours, respectively.

Most noteworthy in Fig. 7 is that, while the early- and late-type galaxies in the green valley exhibit (by selection) similar $u - r$ colours, they have significantly different $NUV - u$ colours. The early-type galaxies exhibit much redder $NUV - u$ colours at the same optical colour than the late types in the (optical) green valley.

This analysis shows that early-type galaxies in the (optical) green valley are quenched rapidly: they show little ongoing star formation while still having significant intermediate-age stellar populations. They feature classic post-starburst stellar populations. The late-type galaxies in the (optical) green valley, on the other hand, show similar $NUV - u$ colours as their star-forming counterparts in the ($u - r$) blue cloud. This is consistent with slowly declining star formation,

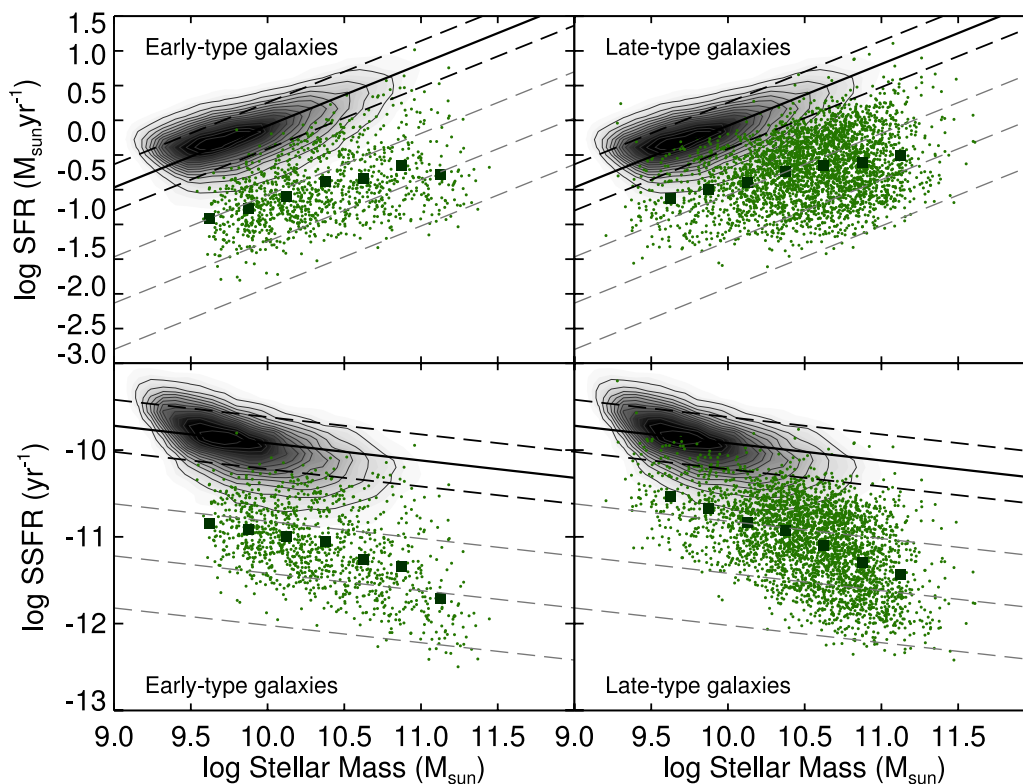


Figure 5. The star formation rate (SFR) and specific star formation rate (sSFR) versus stellar mass diagrams, which highlight the main sequence. In each panel, grey-shaded contours show galaxies classified as star-forming according to the Baldwin, Phillips & Terlevich (1981) emission line diagram (regardless of morphology); lines indicate the main sequence (solid) and 0.3 dex scatter (dashed) with $\beta = -0.2$ (the DR7 β is lower than the DR4 value of -0.1 ; Y. Peng, private communication); the grey dashed lines show further 0.3 dex offsets down from the main sequence. The top row shows the standard SFR versus stellar mass diagram and the bottom row shows the sSFR instead. In the left-hand column, we show the green valley early types as green points and in the right-hand column, we show the green valley late types as green points. The large green squares are median values. For both green valley populations, we plot SFR/sSFRs as reported by the MPA-JHU catalogue regardless of whether the object is classified as star-forming or not (i.e. including upper limits). Both populations are clearly offset from the general population of main-sequence star-forming galaxies – as expected, since they are quenching – and the early types tend to lie further off the main sequence than the late types, especially in the sSFR plot; however, the difference in *optical* colour is small and only UV colours indicate *how fast* galaxies are moving off the main sequence.

so that late types have enough ongoing star formation to still be blue in the ultraviolet, yet the overall stellar population is aging (the mean stellar age is increasing), thus moving them into the optical green valley (and off the main sequence). Indeed, the lack of a green valley in the late-type plot is further evidence for their gradual quenching.

These NUV ur colour–colour diagrams are clearly sensitive diagnostics of young and intermediate age stellar populations, and therefore of recent star formation histories. Using model star formation histories, we can quantify this interpretation and in particular, constrain the time-scales on which star formation declines in the two populations. We construct an illustrative star formation history as follows: a constant SFR for 9 Gyr followed by a transition to an exponentially declining SFR with variable time-scale, τ_{quench} , representing the quenching time-scale. We note that a constant SFR is a reasonable model for a galaxy on the main sequence: despite the fact that the sSFR drops by a factor of ~ 20 from $z \sim 1$ to today, the SFR only changes by about a factor of 3 (Lilly et al. 2013). We discuss the robustness of this model further in Appendix A.

We generate model star formation histories and convolve them with Bruzual & Charlot (2003) population synthesis model spectra to generate a model SED. We blank out the youngest 3 Myr stellar populations to mimic the effect of birth clouds (which obscure the youngest stellar populations), and finally, convolve with filter transmission curves to generate observed colours. We vary τ_{quench} from

1 Myr (effectively instantaneous suppression of star formation) to 2.5 Gyr (a slow decline corresponding a quenching process significantly slower than the dynamical time-scale of a galaxy). The lower-left panel of Fig. 7 shows a schematic of these model star formation histories and the corresponding tracks are overplotted on the NUV ur colour–colour diagrams on the right-hand panels. For each track, we mark 100 Myr intervals with a small point and 1 Gyr intervals with a large point. The $\tau_{\text{quench}} = 1$ Myr track moves rapidly across the diagram within ~ 1 Gyr, while the $\tau_{\text{quench}} = 2.5$ Gyr track barely moves at all in several Gyr; in fact, it never leaves the blue cloud, a point to which we return later.

In Fig. 8, we show using Bruzual & Charlot (2003) models that the value of the time of the quenching event does not matter significantly as the NUV – u colour is strongly dominated by young- and intermediate-age stellar populations in the 10–1500 Myr time range.

We compare these tracks to the observed locations of early- and late-type galaxies on the NUV ur diagram. The early-type galaxies in the green valley are well matched by tracks with very short τ_{quench} . Both the instantaneous truncation track and the track with $\tau_{\text{quench}} = 250$ Myr pass straight through the early-type green valley locus before reaching the red sequence. The $\tau_{\text{quench}} = 1$ Gyr track misses the main early-type locus and in fact stalls in the green valley. If early-type galaxies were quenching as slowly as $\tau_{\text{quench}} = 1$ Gyr,

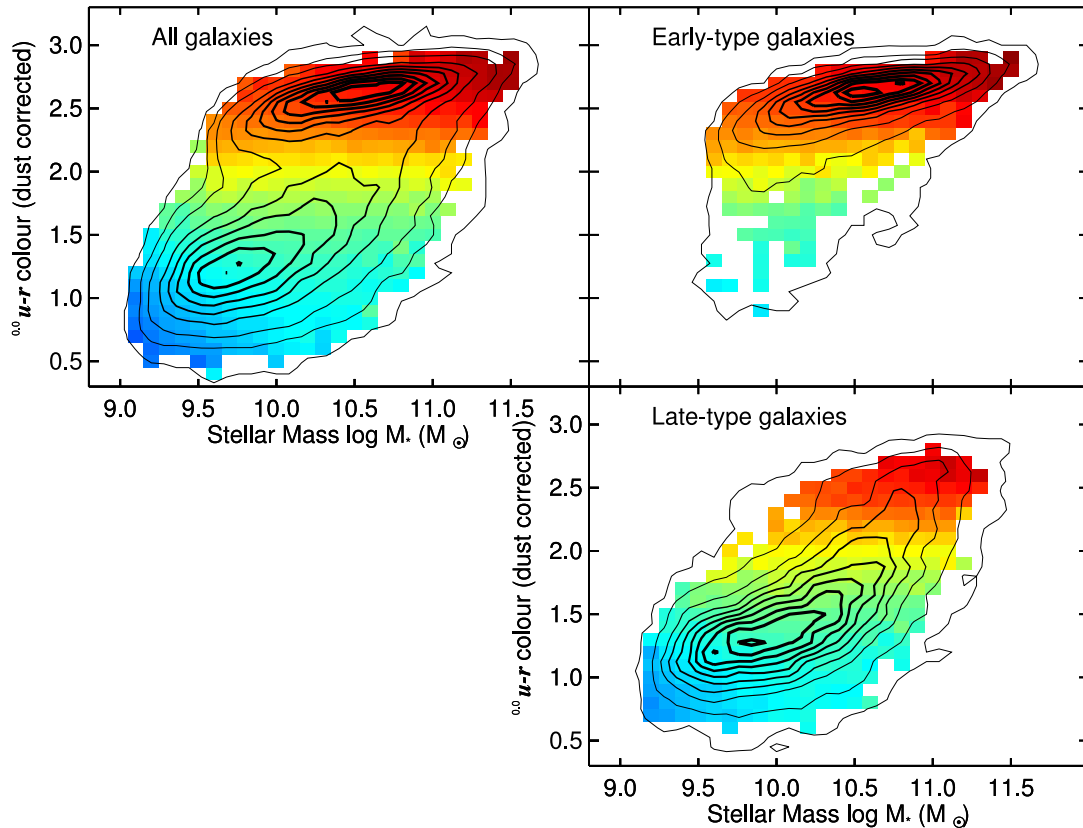


Figure 6. The dust-corrected colour–mass diagram, like Fig. 4 but with the galaxy populations in 0.1×0.1 dex panels coloured by the mean sSFR. This diagram shows that both green valley early- and late-type galaxies have lower sSFRs than their blue cloud counterparts, i.e., they are off the main sequence. Like the SFR/sSFR diagrams in Fig. 5, this figure shows that the (dust-corrected) green valley is populated by off-main-sequence galaxies but *it does not show* how rapidly the sSFRs are declining.

they would build up in the green valley, which is not observed (Fig. 4).

The late-type galaxies in the green valley are inconsistent with most quenching tracks. The $\tau_{\text{quench}} = 1$ Gyr barely goes through the late-type blue cloud locus. Only the $\tau_{\text{quench}} = 2.5$ Gyr track passes through the bulk of the population. This indicates that long quenching time-scales (several Gyr) are required to explain the colour–colour evolution of late types.

We conclude from the NUV ur colour–colour diagram that early- and late-type galaxies follow very different evolutionary pathways to and through the green valley. Early-type galaxies undergo a rapid end to star formation, transiting the green valley rapidly, perhaps as rapidly as stellar evolution allows. By the time they appear in the green valley, most if not all star formation has ceased. Late-type galaxies, in contrast, experience at most a slow decline in star formation and gradual departure from the main sequence. The slowly declining star formation leads to increasingly red optical colours but not necessarily redder UV–optical colours, because extremely young, luminous stars continue to form.

3.4 Caveat: indeterminate-type galaxies

We now revisit the question of the large population of indeterminate-type galaxies (the galaxies that did not receive at least 80 per cent agreement in any morphological category). As is apparent in Fig. 1, most of the indeterminate-types show disc features. In Fig. 9, we show the NUV ur diagram (dust corrected) analogous to Fig. 7, but with the green valley indeterminate-type galaxies overplotted

as green contours. The bulk of the green valley indeterminate types overlap the green valley late-type locus, with somewhat redder colours, with a minority scattering to the early-type locus, no doubt because some of them have big red bulges. The indeterminate types thus mostly quench slowly, similar to the late types, with a minority being misclassified early types, which quench rapidly.

The indeterminate types do not appear to represent an intermediate quenching pathway between the extremes of early- and late-type galaxies. Instead, most follow the late types (likely related to also having a disc), with a minority following the early types, presumably because they are misclassified early types. A more precise investigation of how the indeterminates fit into the general picture presented here will have to rely on future, better imaging data.

3.5 Local environment, halo mass and satellite fraction of galaxies in the green valley

We now investigate whether the environments of early- and late-type galaxies in the green valley can be linked to their very different recent star formation histories. We use the Yang et al. (2007) group catalogue which yields a statistical estimate of the halo mass for each galaxy group, and whether any galaxy is the most massive/luminous in the group (central versus satellite).

In Fig. 10, we show the colour–mass diagram of both early- (top) and late-type (bottom) galaxies split by halo mass (at $M_{\text{halo}} = 10^{12} M_{\odot} h^{-1}$). The value $10^{12} M_{\odot} h^{-1}$ is motivated by previous work on halo quenching (e.g. Cattaneo et al. 2006; Dekel & Birnboim 2006).

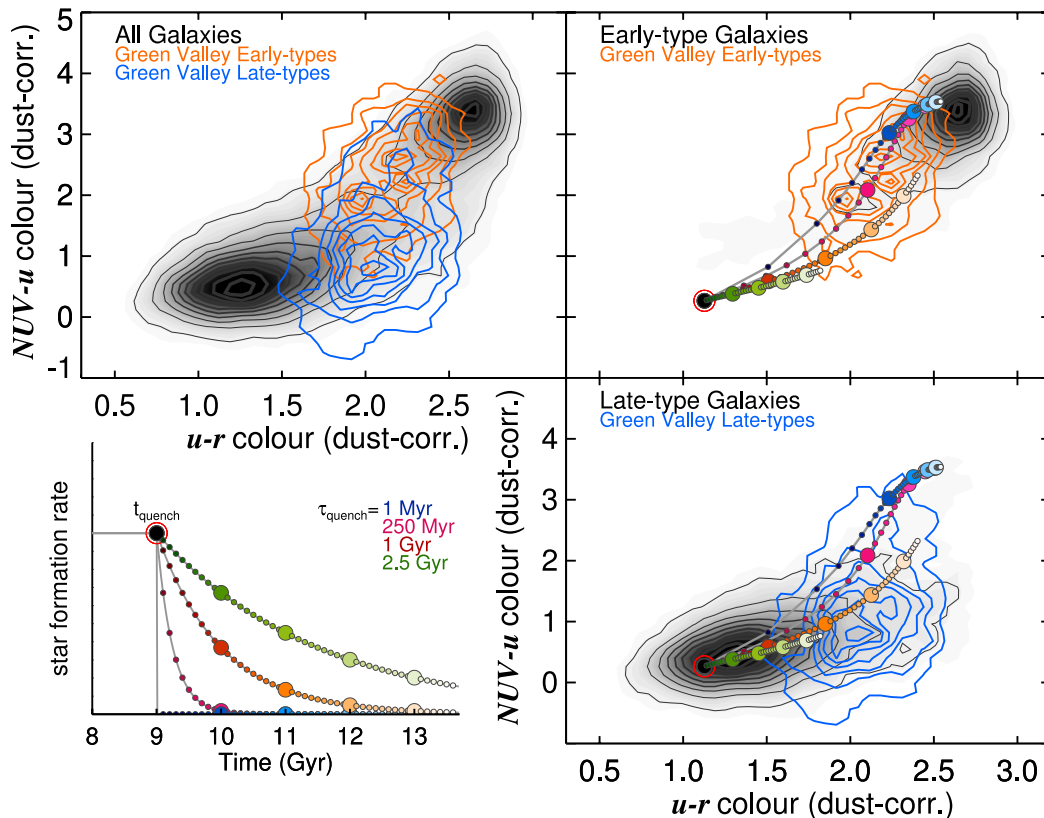


Figure 7. UV–optical colour–colour diagrams (corrected for dust) used to diagnose the recent star formation histories of galaxies. Unlike the sSFR diagrams, these colour–colour diagrams constrain the rate of change in the sSFR, i.e., how rapidly star formation quenches in these galaxies. In each panel, the grey contours represent the underlying galaxy population, while the coloured contours represent galaxies with (optical) green valley colours. In the top-left panel, we show the entire galaxy population and the early- and late-type galaxies in the green valley (orange and blue, respectively). In the right-hand panels, we show only early-type galaxies (top) and only late-type galaxies (bottom). Note that early-type galaxies in the (optical) green valley are significantly redder in $NUV - u$ than late types with the same green valley (optical) colours, indicating they harbour far fewer very young stars. On top of the right-hand panels, we plot a series of evolutionary tracks. Each track follows the same star formation history: constant SFR until, at a time $t_{\text{quench}} = 9$ Gyr, star formation begins to decline exponentially with a quenching time-scale τ_{quench} . The lower-left plot shows four such star formation histories, with an effectively instantaneous τ_{quench} of 1 Myr (blue); more moderate time-scales of 250 Myr (red) and 1 Gyr (orange); and a gentle decline with $\tau_{\text{quench}} = 2.5$ Gyr (green). We overplot these colour-coded evolutionary tracks on the colour–colour diagrams on the right. For each track, we show 100 Myr intervals as small points and 1 Gyr intervals as large points to give a sense of how rapidly galaxies transit the colour–colour diagrams. These diagrams show clearly that the quenching time-scales of early-type galaxies must be very rapid ($\tau_{\text{quench}} \lesssim 250$ Myr), while late-type galaxies must quench very slowly ($\tau_{\text{quench}} > 1$ Gyr).

We find a striking difference between the early- and late-type galaxies. The green valley early-type galaxies are present in both low- and high-mass haloes. The late types show a very dramatic split: the blue cloud (i.e. main sequence) late types are mostly in low-mass haloes, while the green valley and red sequence late types (i.e. partially or mostly quenched) are almost exclusively in high-mass haloes. In other words, early types quench in all environments whereas the quenching in late types is clearly different above and below a halo mass of $10^{12} M_{\odot} h^{-1}$.

Similar results were reported previously by Skibba et al. (2009), who found that late-type quenching is associated with environment, and that late types may be able to quench without an associated morphological transformation. For an in-depth discussion of the stellar mass to halo mass relationship, see Behroozi, Conroy & Wechsler (2010).

3.6 Atomic hydrogen gas in green valley galaxies

We now turn to another aspect of quenching: the gas supply for star formation. Based on the previous sections, we would expect

late-type galaxies in the green valley to retain sizeable reservoirs of gas to sustain ongoing, though slowly declining, star formation, while early-type galaxies should be gas poor to account for a rapid drop in new star formation.

In order to test this hypothesis, we matched our sample to the H I data base from the 40 per cent Arecibo Legacy Fast ALFA Survey (ALFALFA; Haynes et al. 2011). In Table 2, we report the numbers of early- and late-type galaxies in the green valley that were covered and detected in the ALFALFA survey.

We find that 48 per cent of all green valley late-type galaxies were detected in H I by the ALFALFA survey, consistent with many of them retaining significant gas reservoirs. In contrast, only 8 per cent of green valley early-type galaxies were detected in H I, supporting the picture that their star formation was quenched rapidly by removing (or ionizing) the available gas.

On a related note, we have an ongoing program to observe the H I kinematics of green valley early-type galaxies and find that most of them show highly disturbed gas kinematics consistent with having experienced recent mergers (Wong et al., in preparation).

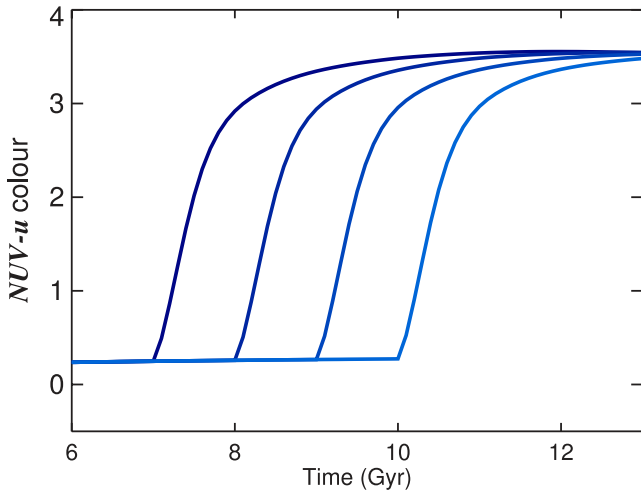


Figure 8. The evolution of the $NUV - u$ colour based on BC03 models following the simple quenching model described in Section 3.3. At some time t_{quench} , a constant SFR star formation history is interrupted and enters an exponential decline with $\tau = 100$ Myr. We vary t_{quench} from 7 to 10 Gyr age to show that the precise quenching time has no significant effect on the $NUV - u$ colour after the rapid (~ 100 Myr) colour transition. This figure illustrates the sensitivity of the $NUV - u$ colour to short time-scales in the 10–1500 Myr range. With a dynamic range of nearly 4 mag, this colour is ideal for tracing quenching time-scales.

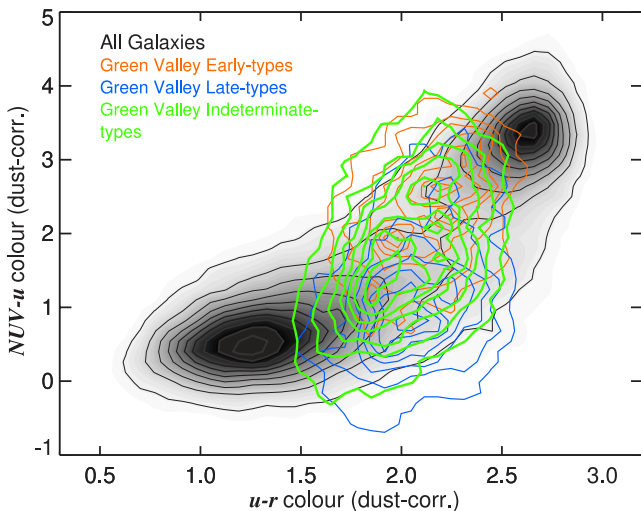


Figure 9. $NUVur$ diagram, similar to the upper-left panel in Fig. 7 but showing the indeterminate-type galaxies as green contours, with early types as orange contours and late types as blue contours. The bulk of the green valley indeterminate types overlap the green valley late-type locus, with somewhat redder colours, with a minority scattering to the early-type locus. This supports a picture where the indeterminate types quenching slowly, similar to the late types, with the minority misclassified early types possibly quenching more rapidly.

Table 2. H I properties of galaxies in the green valley (from 40 per cent ALFALFA data).

Sample	N covered	N detected	N un-detected	H I Detection fraction
Green Valley...				
Early-type Galaxies	349	28	321	8 per cent
Late-type Galaxies	912	435	477	48 per cent

3.7 Black hole growth and galaxies in the green valley

We now turn to the question of how the growth of supermassive black holes in the centres of galaxies might be related to the separate evolutionary pathways for quenching star formation in early- and late-type galaxies. In fact, the present work provides context for interpreting our earlier Galaxy Zoo AGN host galaxy study (Schawinski et al. 2010a).

In Fig. 11, we show the same $NUVur$ colour–colour diagram as in Fig. 7, with emission-line-selected AGN host galaxies added as green points (see Schawinski et al. 2010a for AGN selection details). All AGN are narrow-line Type 2 (obscured) AGN, so there should be no contribution of AGN continuum to the UV/optical colours. Both early- (top right) and late-type (bottom right) AGN host galaxies cluster in the (optical) green valley. This is why it has been suggested previously that black hole accretion is correlated with a decline in sSFR (and therefore green colours; e.g. Schawinski et al. 2007b; Nandra et al. 2007; Wild et al. 2007; Silverman et al. 2008).

Comparing to the evolutionary tracks in Figs 7 and 11, it is clear that in most cases, AGN signatures become visible well past quenching time. We make no assumption on the AGN lifetime here, but consider when, during the evolutionary stage of the host galaxy, black hole accretion is favoured. This delay between the shutdown of star formation and the detection of (emission-line selected) AGN has been noted previously (Davies et al. 2007; Schawinski et al. 2007b, 2009c; Wild et al. 2007); several hundred Myr or more must elapse between the end of star formation in early types and the detection of an optical AGN (Gyr for the late types), even assuming instantaneous quenching (see discussion in Schawinski et al. 2007b, 2009c). This implies that the AGN radiation from green valley early-type galaxies is not responsible for the rapid quenching of star formation seen in them. Rather, the AGN activity is plausibly an after-effect of the event that triggered quenching, rather than its cause.

In late-type galaxies (Fig. 11, bottom right), black hole accretion is visible in the green valley and continues as the galaxy slowly ages to redder colours. The $NUV - u$ colour shows that many late-type galaxies – including the AGN host galaxies – still have young stars (see also Cortese 2012).

These statements are inferred from a sample of emission line-selected AGN; it is important to check whether AGN samples based on other (more inclusive) selections show the same trends.

4 DISCUSSION: EVOLUTIONARY TRACKS RELATED TO THE END OF STAR FORMATION

We have used a series of observational results, informed by morphological classifications, to develop a broad picture of how and why early- and late-type galaxies at $z \sim 0$ transform from blue star-forming galaxies into passively evolving red galaxies. Here, we review the evidence presented in Section 3, then discuss our interpretation.

We first verified that dust extinction, while present, is not the main reason most galaxies have green colours. We then assessed the recent star formation properties of green valley galaxies, as traced by emission lines and by the location of green valley galaxies compared to the main sequence. Both indicators show that low SFRs are the reason green valley galaxies – regardless of morphology – exhibit green optical colours.

We then considered the UV–optical colours of galaxies in the optical ($u - r$) green valley, the UV (from *GALEX*) being more

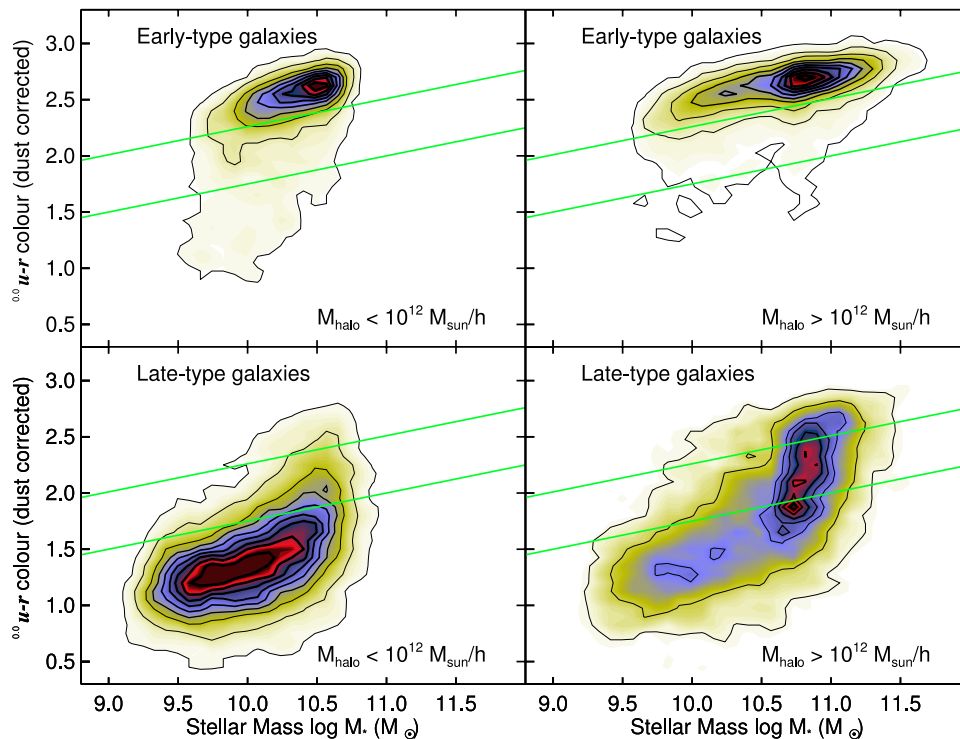


Figure 10. Dust-corrected colour–stellar mass diagrams of early- and late-type galaxies (top- and bottom rows) split by halo mass (from Yang et al. 2007) into low-mass (left) and high-mass haloes (right; split at $M_{\text{halo}} = 10^{12} M_{\odot} h^{-1}$). Only small, qualitative differences are seen in the early-type galaxies, whereas quite striking differences appear in the late types. The green valley early types are present in both low- and high-mass haloes; in low-mass haloes, they are mostly centrals, and in high-mass haloes, mostly satellites. In contrast, the blue cloud late types are mostly in low-mass haloes, while the green valley late types are mostly in massive haloes, and are largely centrals. This makes clear that quenching of star formation in late-type galaxies is closely related to halo mass; those with $M_{\text{halo}} = 10^{12} M_{\odot} h^{-1}$ are partly or mostly quenched, suggesting that accretion of mass through the halo slows or stops above this value.

sensitive to the youngest stars than purely optical colours. We found that, when early-type galaxies are in the (optical) green valley, their UV–optical colours are much redder than those of late-type green valley galaxies. This supports the idea that the two morphological classes have fundamentally different recent star formation histories (i.e. different UV– u colours), even after the initial stellar populations have aged in a similar way (i.e. optical colours are green). We used model evolutionary tracks to show that this difference corresponds to very different time-scales on which star formation declines: in early-type galaxies, the quenching time-scale is much shorter (< 250 Myr) than in late-type galaxies (> 1 Gyr).

All this evidence leads to a coherent physical picture where a quenching event destroys the (quasi) equilibrium state of main-sequence star-forming galaxies, moving them off the main sequence into the green valley. The data clearly show that the time-scale for this colour evolution is strongly tied to morphology. We now argue that two quenching pathways – for early-type and for late-type galaxies – can be tied to two different scenarios for destroying gas reservoirs, i.e., to two different physical quenching mechanisms. Because most star-forming galaxies start on the main sequence of star formation, where a simple regulator balances cosmological inflows of gas with outflows (Lilly et al. 2013), we take the main sequence as the starting point of the evolutionary models discussed below.

4.1 The evolution of late-type galaxies

We have shown that the star formation histories of late-type galaxies are consistent with a very gradual quenching, corresponding to an

exponential time-scale of a Gyr or more. A natural explanation is that the baryon supply is disrupted, so that the SFR declines slowly in response to the depletion of the gas reservoir. The disruption could be due to halo mass quenching (e.g. Cattaneo et al. 2006), the end of cold streams and the development of a hot halo due to shocks (Dekel & Birnboim 2006; Dekel et al. 2009), or simply the continued expansion of the virial radius to a point where cooling from the halo to the disc becomes inefficient (i.e. too slow). While other environmental processes may also play a role – for example, ram pressure, stripping or harassment (see Tonnesen 2011 and Vollmer 2013 for recent reviews) – these local considerations cannot explain the global behaviour of late-type galaxies as a class.

The rate at which star formation exhausts gas can be written in a dynamical form as (Guiderdoni et al. 1998; Hatton et al. 2003; Kaviraj et al. 2011):

$$\psi = \frac{\epsilon M_{\text{gas}}}{\tau_{\text{dyn}}}, \quad (3)$$

where ψ is the SFR, M_{gas} is the gas reservoir available for star formation, τ_{dyn} is the dynamical time-scale, and ϵ is the (fixed) efficiency of star formation (we assume the universal value $\epsilon = 2$ per cent; e.g. Kennicutt 1998). The dynamical time-scale for the disc of a massive galaxy is of the order of $\tau_{\text{dyn}} \sim 50$ – 300 Myr. The mass of the gas reservoir is a free parameter set by the initial conditions. Once the initial gas reservoir is specified and a reasonable dynamical time-scale is chosen, equation 3 can be solved to describe the evolution of the system. The e-folding time for the declining SFR

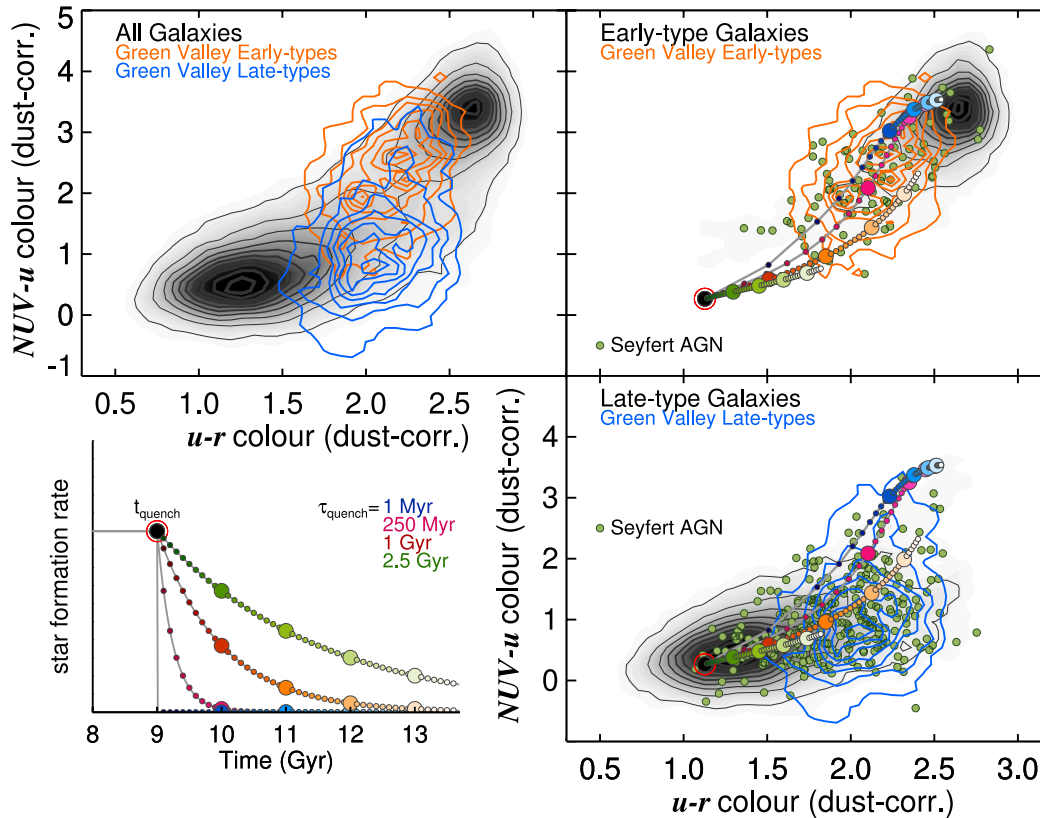


Figure 11. NUV u diagram, same as Fig. 7, but showing the emission line-selected AGN host galaxies as green points. This diagram places these AGN host galaxies in the context of quenching scenarios: both early-type and late-type AGN hosts lie squarely in the (optical) green valley, a few hundred Myr or longer after the quenching event. In both cases, the AGN identified via emission lines cannot be responsible for the quenching, as they appear several hundred Myr along the quenching tracks.

is $\tau_{\text{dyn}}/\epsilon$, which is several Gyr for the adopted parameters.⁵ That is, galaxies with a gas reservoir that does not get replenished from outside will continue to form stars for a very long time, peeling off from the main sequence of star formation very slowly, as previously argued by Kaviraj et al. (2011). In Fig. 12, we show how the sSFR, $u - r$ colours, and gas fractions evolve according to equation (3) for a range of quenching time-scales.

The evolution of late-type galaxies corresponds to the longer time-scale tracks in Fig. 12. This means there is enough time to develop a significant population of late types in the green valley and, eventually, the red sequence. Late-type galaxies in the green valley should still have substantial gas reservoirs that fuel ongoing star formation. Initial data from H I data support this (Section 3.6).

The start of quenching may occur at (very) high redshift, as it can take several Gyr for the effects of a slowly declining SFR to become apparent. In this context, red spirals (e.g. van den Bergh 1976; Wolf et al. 2009; Masters et al. 2010b) are simply late-type galaxies whose cutoff happened relatively early and their discs might start fading (Carollo et al. 2014). The observation of Masters et al. (2010b) and Cortese (2012) that red spirals still show signs of low-level star formation make sense – they are simply very far along the exponential decline in SFR off the main sequence.

⁵ This time-scale for gas depletion corresponds to what happens in the ‘bathtub’ model of Lilly et al. (2013) when the gas supply to the reservoir is shut off.

The reddest colours in late-type galaxies preferentially occur in high-mass haloes (Fig. 10), supporting the suggestion that the gas supply is somehow regulated by environmental factors. Of course, other factors besides halo mass can increase the pace of gas depletion following the original quenching event – and this must happen. Fig. 7 shows some objects with quenching time-scales slightly shorter than that expected from canonical parameters.

For example, bars naturally shorten gas consumption time-scales, by driving gas into the central regions of galaxies where it can be consumed more quickly. Masters et al. (2011, 2012) found that the incidence of bars in massive late-type galaxies increases as they become redder. This could be a side effect of quenching – models show that bars form more quickly in gas-poor discs (e.g. Athanassoula, Machado & Rodionov 2013) – but if secular evolution along a bar is an efficient process, the presence of a bar could also speed up the quenching time such that the transition happens more rapidly than the several Gyr expected from the simple Schmidt law. Masters et al. (2012) show that high bar fractions in spirals are associated with lower H I gas content, and there are hints that at a fixed H I content barred galaxies are optically redder than unbarred galaxies. Several works (Sheth et al. 2008; Cameron et al. 2010; Melvin et al. 2014) show that the fraction of disc galaxies with bars also seems to have been increasing since $z \sim 1$ Sheth et al. (2008); Cameron et al. (2010). Thus, secular processes like bar formation may be intimately tied to quenching in late-type galaxies; even if they appear after the initial quenching event, they would help drive out the remaining gas reservoir, thus accelerating the rate at which late types become fully gas- and star formation free.

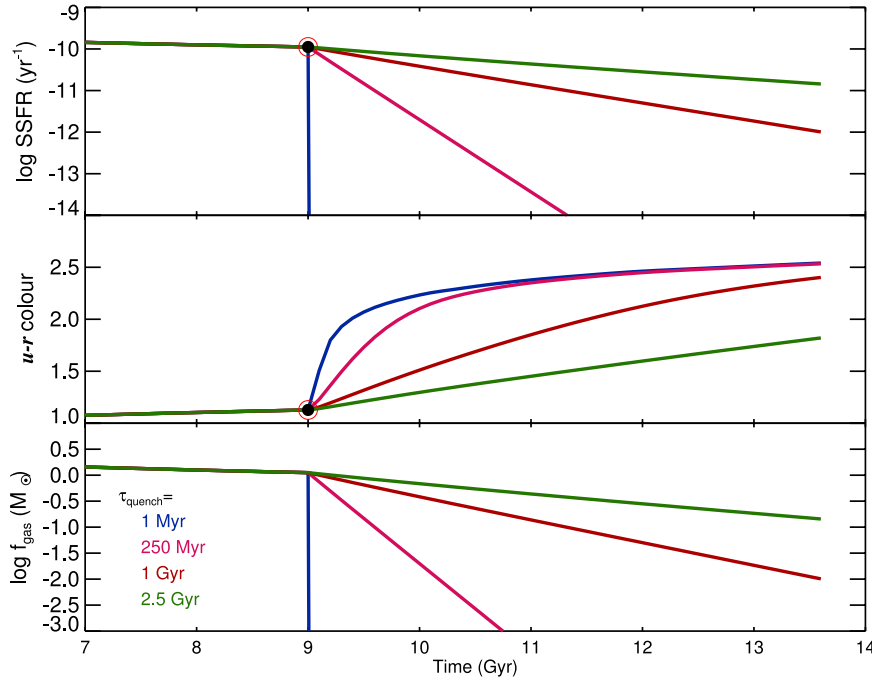


Figure 12. Diagram showing the evolution of a galaxy corresponding to the quenching scenarios discussed in the text. The SFR is constant until quenching begins at $t = 9$ Gyr, then declines exponentially with $\tau_{\text{quench}} \in \{1, 250, 1000, 2500\}$ Myr. (*Top panel:*) evolution of the sSFR; (*middle panel:*) $u - r$ colour evolution; (*bottom panel:*) gas fraction, inferred from the SFR by inverting the Schmidt law (equation 3).

Environment as a late-stage accelerator or modifier of quenching is naturally supported by the strong effect of halo mass on the presence of green and red late types (Section 3.5). Other recent observational studies have argued that environment or satellite quenching should act fast, at least once it begins (e.g. Muzzin et al. 2012; Wetzel et al. 2013).

Other environmental effects can accelerate the quenching process by further removing gas but not too quickly, as we do not see late-type galaxies with short quenching time-scales. We note that these modulating effects (secular processes and environment) mean that most likely we cannot accurately reconstruct the time of quenching for present-day green and red (i.e. off-main sequence) late types.

Now we consider the possible role of AGN feedback in the evolution of late-type galaxies. The majority of black holes growing locally and at high redshift are hosted in late-type galaxies, clearly driven by secular processes rather than major mergers (e.g. Schawinski et al. 2010a, 2011, 2012; Cisternas et al. 2011; Kovcevski et al. 2012; Simmons et al. 2012; Treister et al. 2012). The fraction of green valley galaxies that host AGN is higher than in blue star-forming galaxies (Fig. 11). This could be due in part to an observational bias (the difficulty of seeing AGN signatures in SDSS spectra against a more luminous stellar component), but sensitive multiwavelength searches for ‘missed’ AGN in nearby star-forming galaxies (e.g. Goulding et al. 2010) do not find enough to balance the numbers. Moreover, hard X-ray selection should not be confused by star formation, yet this technique also detects few to no (high luminosity) AGN in the blue cloud (Schawinski et al. 2009c). We conclude the prevalence of AGN in green valley galaxies is likely real rather than a selection effect.

The alternative is that the onset of quenching in late-type galaxies leads to increased black hole growth about 1 Gyr later. The delay could be explained naturally by the time required for accreting matter to lose angular momentum. In this case, black hole feeding would be due to secular processes (since major mergers would dis-

rupt the disc morphology) and could not significantly speed up the quenching (or the AGN hosts would transition much more rapidly across NUV ur colour space); it would be a consequence of the host galaxy quenching, not the cause. Perhaps a declining sSFR favours black hole growth: Davies et al. (2007) suggested that the absence of strong stellar feedback (core collapse supernovae, O-star winds) makes it easier to transport gas to the centre, and also that mass-loss from Asymptotic Giant Branch stars could easily fuel black hole accretion because of both the larger amount of material and its lower velocity.

Peng et al. (2010) identified two distinct quenching mechanisms at work in galaxies: environment and mass quenching (without identifying the physical mechanisms). From the data presented in Section 3.5, one might speculate that early-type galaxies are mass quenched (no strong dependence on environment) and late types are environment quenched (strong dependence on environment). A test of this hypothesis would be the mass functions of green valley early- and late-type galaxies: if the quenching pathway we identify in early types is mass quenching (see below), then the green valley early types should have the same mass function as the passive galaxies (in terms of M_* and faint end slope α_s , the normalization Φ_* will depend on transition time-scale); similarly, if the quenching pathway we identify in late types is environment quenching, then the green valley late types should have the same mass function as the star-forming galaxies.

4.2 The evolution of early-type galaxies

The end of star formation in early-type galaxies in the local Universe proceeds in a fundamentally different fashion than in the late-type galaxies. In local early types, quenching occurs in low-mass galaxies and is marked by a very rapid shutdown of star formation on time-scales consistent with instantaneous suppression, or at most $\tau_{\text{quench}} \sim 250$ Myr (cf. Schawinski et al. 2007b). This rapid

suppression is inconsistent with the simple gas exhaustion scenario outlined for late-type galaxies; the Schmidt law does not allow star formation to deplete a substantial gas reservoir so rapidly (a point made strongly by Kaviraj et al. 2011). The quenching mechanism should also be linked to the destruction of the disc morphology of the likely progenitor(s).

A major merger (Schawinski et al. 2010b) could simultaneously transform the galaxy morphology from disc to spheroid and cause rapid depletion of the cold gas reservoir. Deep imaging of blue early types does reveal tidal features indicative of a major merger (Schawinski et al. 2010b) but Wong et al. (2012) have shown that galaxies with post-starburst spectral features already have early-type morphologies, emphasizing that the morphological transformation must be rapid.

Studies of gas kinematics (molecular, ionized) show that most early-type galaxies, and specifically those in the green valley, have gas with an external origin, most likely due to merger activity (Sarzi et al. 2006; Shapiro et al. 2010; Davis et al. 2013; Khochfar & Burkert 2003). These blue precursors must have similar masses but bluer (intrinsic) colours than the AGN early-type hosts (see Fig. 4 and Schawinski et al. 2007b, 2009a). Observations of a small sample of early types along this evolutionary path from the blue cloud to the red sequence shows that the large molecular gas reservoirs of blue early-type galaxies do disappear rapidly, at a rate significantly faster than can be explained by star formation alone (Schawinski et al. 2009b).

We note that, as with the green valley late types, the quenching event – i.e. the point at which the gas fuelling star formation was destroyed – had to occur before the galaxy reaches the green valley. Given the short time between quenching and arrival in the green valley (only a few hundred Myr), it may be easier to identify this progenitor population than in late types. So far, Schawinski et al. (2009b) found that green valley (Seyfert AGN) early-type galaxies were undetected in molecular gas and that the gas disappeared rapidly during the transition from purely star-forming to an AGN+star formation mixed phase.

Naturally, today’s galaxies host both stellar populations formed in situ and those brought in via progenitors in minor and major mergers. In this general picture, star formation in early-type galaxies ceases and then does not re-start except for a minor frosting of new stellar populations (seen mostly in the ultraviolet; e.g. Yi et al. 2005; Kaviraj et al. 2007; Schawinski et al. 2007a), except when a new disc forms through the acquisition of a sufficient supply of cold gas, at which point the galaxy would rejoin the main sequence.

What about the role of AGN feedback? Rapid depletion of a large fraction of the available gas could be caused by a vigorous starburst, as star formation uses up cold gas and stellar processes create strong winds. Simulations show that merger-induced starbursts can lead to enhanced star formation as disc destruction leads to the inflow of gas to the (new) galaxy centre, all on relatively short dynamical time-scales (e.g. Barnes & Hernquist 1996). However, in this starburst-induced scenario, even a short depletion time-scale will still yield a remnant system that is not entirely quenched. The Schmidt law forces the star formation back to an exponentially decaying state, albeit with a shorter time-scale, which in turn means that the galaxy retains gas, and therefore continues forming stars. Only by adding AGN feedback, which can destroy the gas reservoir, do simulations show a genuine total quenching of star formation (e.g. Springel, Di Matteo & Hernquist 2005).

Is it possible that AGN feedback alone destroys the gas reservoir during merger? It is true that photoionization happens almost

instantaneously, so a luminous AGN could destroy the cold gas reservoir almost instantaneously. However, we would then expect detectable AGN radiation before the host galaxies reach the green valley, while they are still in the blue, star-forming phase, contrary to what is observed (Schawinski et al. 2009c; Goulding et al. 2010). If AGN feedback were responsible for the rapid gas reservoir destruction, then during this phase it must be either very short-lived, heavily obscured or radiatively inefficient (Schawinski et al. 2009b; Schawinski 2012).

A radiatively inefficient accretion flow could drive a kinetic outflow (jet, disc wind or other outflow), analogous to what X-ray binaries do (e.g. Maccarone, Gallo & Fender 2003; K rding, Jester & Fender 2006; McHardy et al. 2006; Pakull, Soria & Motch 2010). In this early phase, the AGN would be outshone by the declining starburst; the place to look for evidence of this kind of kinetic feedback would be at the transition from star-forming to composite spectrum in the blue early-type galaxy population.

We note that dwarf ellipticals are not in our sample and their quenching pathways may be very different (e.g. Boselli et al. 2008).

5 SUMMARY

We have used new morphological analyses from Galaxy Zoo to map out the evolutionary pathways of local galaxies. We showed that the paths taken by late-type and early-type galaxies through the (optical) green valley are quite different, and that their quenching mechanisms have very different time-scales. This means that thinking of the green valley as a transition phase for all (or even most) galaxies is overly simple. In particular, late-type galaxies do not exhibit the colour bimodality seen in the colour–mass or colour–magnitude diagrams of the total galaxy population.

From a detailed analysis of sSFR, dust-corrected UV–optical colours and other properties, we traced the evolution of early- and late-type galaxies through the green valley. Both leave the main sequence and enter the green valley as their sSFR drops, but they do so with very different rates of change. UV–optical colours show that the rate of change in sSFR (d/dt sSFR) – i.e. the quenching time-scale – is rapid in early-type galaxies ($\tau < 250$ Myr), while late-type galaxies undergo a much more gradual decline in star formation ($\tau > 1$ Gyr). We illustrate these morphology-related star formation quenching pathways with cartoons in Figs 13 and 14, as described here.

Late-type galaxies

(i) The quenching of star formation is initiated by a cutoff of the galaxy gas reservoir from the cosmic supply of fresh gas. This cutoff could be due, for example, to the halo mass reaching $10^{12} M_{\odot}$, preventing further accretion of gas on to the galaxy, or to cooling of the hot halo gas becoming inefficient.

(ii) This disturbance of the balance of inflows and outflows moves the galaxy off the main sequence, as star formation uses up the remaining gas and the gas reservoir is not replenished. Where initially the galaxy SFR scales nearly linearly with the stellar mass (the main sequence), it then declines exponentially after quenching commences, with a long characteristic time-scale that to first order is set by the gas reservoir at the time quenching begins and the dynamical time-scale of the galaxy disc.

(iii) Since the SFR is declining, but not zero, the stellar mass may continue to increase as star formation converts the remaining gas reservoir to stars.

Late-type galaxy star formation quenching schematic

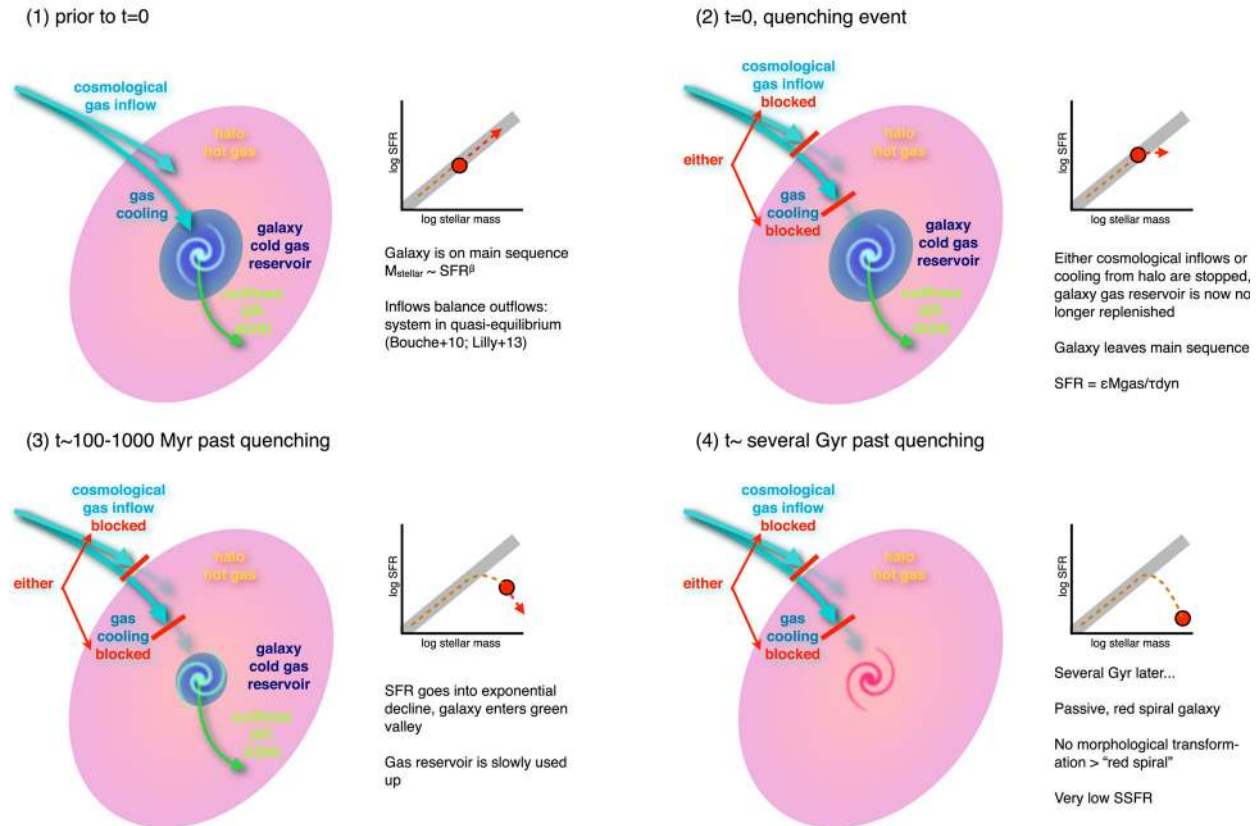


Figure 13. Diagram outlining the scenario presented here for star formation quenching in late-type galaxies. Once the external supply of gas to the galaxy's reservoir is cut off, the galaxy will leave the main sequence, and the SFR will decay exponentially, with a long quenching time-scale τ_{quench} . While no longer on the main sequence, the galaxy nevertheless continues to convert gas to stars and thus to increase its stellar mass. Absent a major merger, this evolutionary pathway eventually produces a passive, red, late-type galaxy. We see radiation from black hole growth during stage (3), long after the quenching event actually took place.

(iv) The galaxy moves slowly out of the blue cloud and into the green valley. Objects that were quenched this way at high redshift may by now have reached the red sequence, accounting for the red population.

(v) The gas-depletion process can be accelerated by other physical processes, in particular secular processes and environmental processes.

(vi) Black hole accretion appears to be favoured in late types that have been quenched and are in the exponential decline phase.

(vii) Observations of still-significant gas reservoirs and high dark matter halo masses support this evolutionary scenario.

(viii) The time delay between the quenching event (i.e. the point at which the external gas supply to the galaxy reservoir is cut off) and the time that the quenching becomes apparent (by movement out of the blue cloud and into the green valley) is long, of the order of several Gyr. This means that studying the local green valley galaxies will not allow us to understand this quenching mode or directly observe it in action. It also means that the green and red late types we see today may be amongst the first to have quenched. The Milky Way may be on a similar trajectory to quiescence.

Early-type galaxies

(i) The quenching of star formation is triggered by the rapid destruction of the galaxy gas reservoir. This must occur

rapidly and cannot be due to gas exhaustion by star formation alone.

(ii) The destruction of the gas reservoir triggers the immediate departure from the main sequence of the galaxy. The SFR rapidly approaches zero, which means the galaxy no longer increases its stellar mass.

(iii) The drop in SFR corresponds to the galaxy moving out of the blue cloud, into the green valley and to the red sequence as fast as stellar evolution allows. The transition process in terms of galaxy colour takes about 1 Gyr.

(iv) The rapid quenching event is effectively simultaneous with the morphological transformation, since there are very few blue early-type galaxies. This suggests a common origin in a major merger.

(v) Visible radiation from black hole accretion is associated with the green valley, i.e. only *after* the quenching event.

(vi) The rapidity of the gas reservoir destruction suggests that unusually strong stellar process and/or AGN feedback (winds, ionization) are involved, perhaps in a kinetic or highly obscured phase.

(vii) To understand the physics of quenching in early types more fully requires observations of the progenitors of the blue early types – most likely major, gas-rich mergers – where we can see which processes (AGN or not) destroy the gas reservoir.

Early-type galaxy star formation quenching schematic

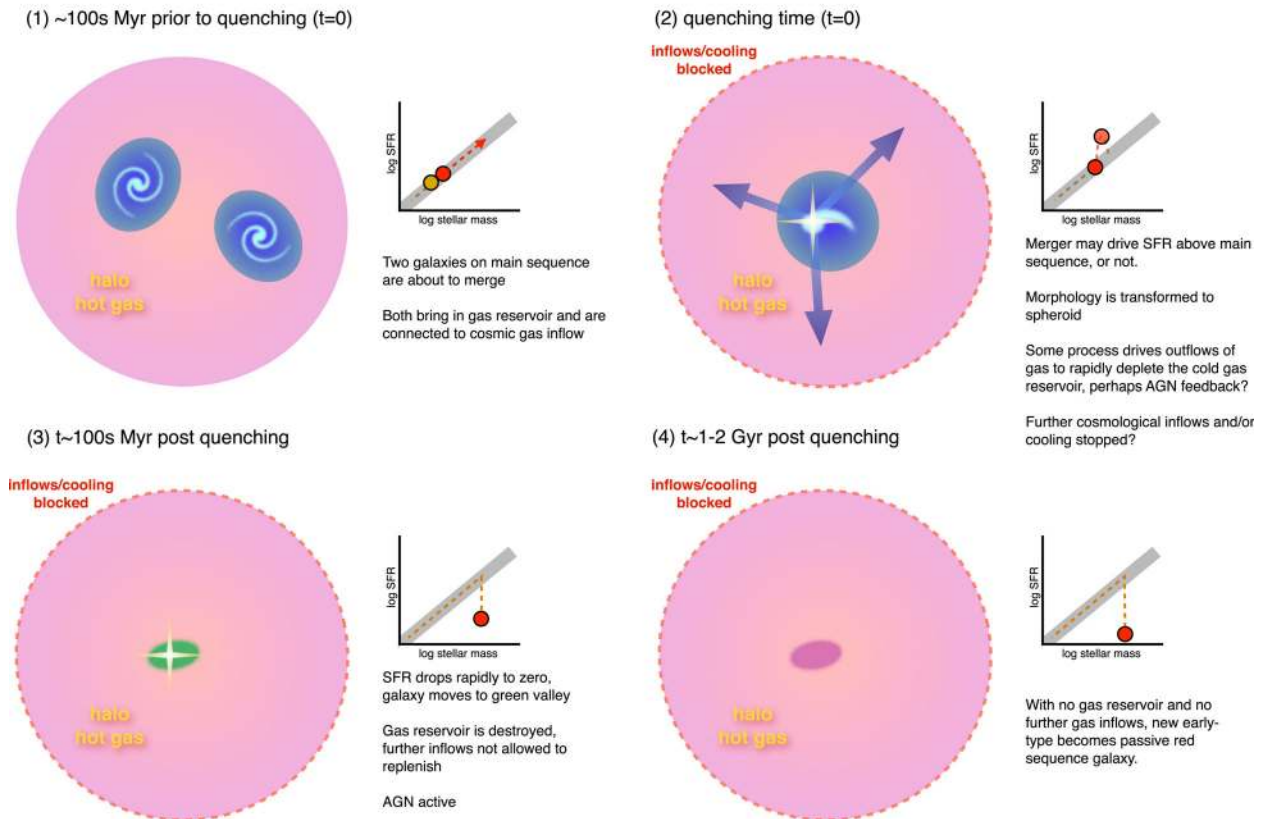


Figure 14. Diagram outlining the scenario presented here for star-formation quenching in early-type galaxies. A dramatic event, likely a gas-rich merger of main sequence star-forming galaxies, causes the near-instantaneous destruction of the (newly formed) early-type galaxy gas reservoir, via stellar processes and/or AGN feedback. As long as the gas reservoir is not resupplied or the AGN keeps the gas hot, star formation ceases and no further stellar mass is formed. An AGN phase is visible for hundreds of Myr as the stars in the early-type host galaxy age rapidly through the green valley.

ACKNOWLEDGEMENTS

We thank C. M. Carollo, S. Lilly, E. Bell and Y. Peng for useful discussions and A. Muench for help with the VO. We also thank the anonymous referee for helpful comments.

KS gratefully acknowledges support from Swiss National Science Foundation Grant PP00P2_138979/1. BDS acknowledges support from the Oxford Martin School and Worcester College, Oxford. The development of Galaxy Zoo was supported by a Jim Gray grant from Microsoft and The Leverhulme Trust. RCN acknowledges STFC Rolling Grant ST/I001204/1 ‘Survey Cosmology and Astrophysics’. SKY acknowledges the support from the National Research Foundation of Korea to the Center for Galaxy Evolution Research (No. 2010-0027910) and Korea Research Council of Fundamental Science and Technology (DRC Program, FY 2012). Support for the work of ET was provided by the Center of Excellence in Astrophysics and Associated Technologies (PFB 06), by the FONDECYT grant 1120061 and the Anillo project ACT1101. LFF and KWW acknowledge support the US National Science Foundation under grant DRL-0941610. RAS is supported by the NSF grant AST-1055081. SK acknowledges a Senior Research Fellowship from Worcester College, Oxford. All hail the Glow Cloud.

Galaxy Evolution Explorer (GALEX) is a NASA Small Explorer, launched in 2003 April. We gratefully acknowledge NASA’s support for construction, operation and science analysis for the

GALEX mission, developed in cooperation with the Centre National d’Etudes Spatiales of France and the Korean Ministry of Science and Technology.

This publication makes use of data products from the Two Micron All Sky Survey, which is a joint project of the University of Massachusetts and the Infrared Processing and Analysis Center/California Institute of Technology, funded by the National Aeronautics and Space Administration and the National Science Foundation.

Funding for the SDSS and SDSS-II has been provided by the Alfred P. Sloan Foundation, the Participating Institutions, the National Science Foundation, the US Department of Energy, the National Aeronautics and Space Administration, the Japanese Monbukagakusho, the Max Planck Society and the Higher Education Funding Council for England. The SDSS web site is <http://www.sdss.org/>.

The SDSS is managed by the Astrophysical Research Consortium for the Participating Institutions. The Participating Institutions are the American Museum of Natural History, Astrophysical Institute Potsdam, University of Basel, University of Cambridge, Case Western Reserve University, University of Chicago, Drexel University, Fermilab, the Institute for Advanced Study, the Japan Participation Group, Johns Hopkins University, the Joint Institute for Nuclear Astrophysics, the Kavli Institute for Particle Astrophysics and Cosmology, the Korean Scientist Group, the Chinese Academy of Sciences (LAMOST), Los Alamos National

Laboratory, the Max-Planck-Institute for Astronomy (MPIA), the Max-Planck-Institute for Astrophysics (MPA), New Mexico State University, Ohio State University, University of Pittsburgh, University of Portsmouth, Princeton University, the United States Naval Observatory and the University of Washington.

This publication made extensive use of the Tool for OPERations on Catalogues And Tables (TOPCAT, which can be found at <http://www.starlink.ac.uk/topcat/>). This research has made use of NASA's ADS Service.

REFERENCES

- Abazajian K. N. et al., 2009, *ApJS*, 182, 543
- Athanassoula E., Machado R. E. G., Rodionov S. A., 2013, *MNRAS*, 429, 1949
- Baldry I. K., Glazebrook K., Brinkmann J., Ivezić Ž., Lupton R. H., Nichol R. C., Szalay A. S., 2004, *ApJ*, 600, 681
- Baldry I. K., Balogh M. L., Bower R. G., Glazebrook K., Nichol R. C., Bamford S. P., Budavari T., 2006, *MNRAS*, 373, 469
- Baldwin J. A., Phillips M. M., Terlevich R., 1981, *PASP*, 93, 5
- Bamford S. P. et al., 2009, *MNRAS*, 393, 1324
- Barnes J. E., Hernquist L., 1996, *ApJ*, 471, 115
- Behroozi P. S., Conroy C., Wechsler R. H., 2010, *ApJ*, 717, 379
- Bell E. F. et al., 2004, *ApJ*, 608, 752
- Blanton M. R., Roweis S., 2007, *AJ*, 133, 734
- Blanton M. R. et al., 2005, *AJ*, 129, 2562
- Boselli A., Boissier S., Cortese L., Gavazzi G., 2008, *ApJ*, 674, 742
- Bouché N. et al., 2010, *ApJ*, 718, 1001
- Brammer G. B. et al., 2009, *ApJ*, 706, L173
- Brinchmann J., Charlot S., White S. D. M., Tremonti C., Kauffmann G., Heckman T., Brinkmann J., 2004, *MNRAS*, 351, 1151
- Bruzual G., Charlot S., 2003, *MNRAS*, 344, 1000
- Calzetti D., Armus L., Bohlin R. C., Kinney A. L., Koornneef J., Storchi-Bergmann T., 2000, *ApJ*, 533, 682
- Cameron E. et al., 2010, *MNRAS*, 409, 346
- Cappellari M., Emsellem E., 2004, *PASP*, 116, 138
- Cardamone C. et al., 2009, *MNRAS*, 399, 1191
- Cardamone C. N., Urry C. M., Schawinski K., Treister E., Brammer G., Gawiser E., 2010, *ApJ*, 721, L38
- Cardelli J. A., Clayton G. C., Mathis J. S., 1989, *ApJ*, 345, 245
- Carollo C. M. et al., 2012, *ApJ*, 776, 71
- Carollo C. M. et al., 2014, *ApJ*, preprint ([arXiv:1402.1172](https://arxiv.org/abs/1402.1172))
- Cattaneo A., Dekel A., Devriendt J., Guiderdoni B., Blaizot J., 2006, *MNRAS*, 370, 1651
- Cheung E. et al., 2013, *ApJ*, 779, 162
- Cibinel A. et al., 2012, *ApJ*, 777, 116
- Cimatti A. et al., 2013, *ApJ*, 779, L13
- Cisternas M. et al., 2011, *ApJ*, 726, 57
- Cortese L., 2012, *A&A*, 543, A132
- Darg D. W. et al., 2010a, *MNRAS*, 401, 1043
- Darg D. W. et al., 2010b, *MNRAS*, 401, 1552
- Davies R. I., Müller Sánchez F., Genzel R., Tacconi L. J., Hicks E. K. S., Friedrich S., Sternberg A., 2007, *ApJ*, 671, 1388
- Davis T. A. et al., 2013, *MNRAS*, 429, 534
- Dekel A., Birnboim Y., 2006, *MNRAS*, 368, 2
- Dekel A. et al., 2009, *Nature*, 457, 451
- Elbaz D. et al., 2007, *A&A*, 468, 33
- Elbaz D. et al., 2011, *A&A*, 533, A119
- Faber S. M. et al., 2007, *ApJ*, 665, 265
- Gonçalves T. S., Martin D. C., Menéndez-Delmestre K., Wyder T. K., Koeke-moer A., 2012, *ApJ*, 759, 67
- Goulding A. D., Alexander D. M., Lehmer B. D., Mullaney J. R., 2010, *MNRAS*, 406, 597
- Guiderdoni B., Hivon E., Bouchet F. R., Maffei B., 1998, *MNRAS*, 295, 877
- Hasinger G., 2008, *A&A*, 490, 905
- Hatton S., Devriendt J. E. G., Ninin S., Bouchet F. R., Guiderdoni B., Vibert D., 2003, *MNRAS*, 343, 75
- Haynes M. P. et al., 2011, *AJ*, 142, 170
- Hoyle B. et al., 2011, *MNRAS*, 415, 3627
- Kauffmann G. et al., 2003, *MNRAS*, 341, 33
- Kaviraj S. et al., 2007, *ApJS*, 173, 619
- Kaviraj S., Schawinski K., Silk J., Shabala S. S., 2011, *MNRAS*, 415, 3798
- Kaviraj S., Darg D., Lintott C., Schawinski K., Silk J., 2012, *MNRAS*, 419, 70
- Keel W. C. et al., 2012, *MNRAS*, 420, 878
- Kennicutt R. C., Jr, 1998, *ApJ*, 498, 541
- Khochfar S., Burkert A., 2003, *ApJ*, 597, L117
- Kocevski D. D. et al., 2012, *ApJ*, 744, 148
- Komatsu E. et al., 2011, *ApJS*, 192, 18
- Körding E. G., Jester S., Fender R., 2006, *MNRAS*, 372, 1366
- Land K. et al., 2008, *MNRAS*, 388, 1686
- Lee K.-S. et al., 2012, *ApJ*, 752, 66
- Leitner S. N., 2012, *ApJ*, 745, 149
- Lilly S. J., Carollo C. M., Pipino A., Renzini A., Peng Y., 2013, *ApJ*, 772, 119
- Lintott C. J. et al., 2008, *MNRAS*, 389, 1179
- Lintott C. J. et al., 2009, *MNRAS*, 399, 129
- Lintott C. et al., 2011, *MNRAS*, 410, 166
- Maccarone T. J., Gallo E., Fender R., 2003, *MNRAS*, 345, L19
- Martin D. C. et al., 2005, *ApJ*, 619, L1
- Martin D. C. et al., 2007, *ApJS*, 173, 342
- Masters K. L. et al., 2010a, *MNRAS*, 404, 792
- Masters K. L. et al., 2010b, *MNRAS*, 405, 783
- Masters K. L. et al., 2011, *MNRAS*, 411, 2026
- Masters K. L. et al., 2012, *MNRAS*, 424, 2180
- McHardy I. M., Koerding E., Knigge C., Uttley P., Fender R. P., 2006, *Nature*, 444, 730
- Melvin T. et al., 2014, *MNRAS*, 438, 2882
- Mendez A. J., Coil A. L., Lotz J., Salim S., Moustakas J., Simard L., 2011, *ApJ*, 736, 110
- Muzzin A. et al., 2012, *ApJ*, 746, 188
- Muzzin A. et al., 2013, *ApJ*, 777, 18
- Nandra K. et al., 2007, *ApJ*, 660, L11
- Noeske K. G. et al., 2007, *ApJ*, 660, L43
- Oh K., Sarzi M., Schawinski K., Yi S. K., 2011, *ApJS*, 195, 13
- Padmanabhan N. et al., 2008, *ApJ*, 674, 1217
- Pakull M. W., Soria R., Motch C., 2010, *Nature*, 466, 209
- Peng Y.-j. et al., 2010, *ApJ*, 721, 193
- Salim S. et al., 2007, *ApJS*, 173, 267
- Sarzi M. et al., 2006, *MNRAS*, 366, 1151
- Schawinski K., 2009, in Heinz S., Wilcots E., eds, *AIP Conf. Ser. Vol. 1201, The Monster's Fiery Breath: Feedback in Galaxies, Groups, and Clusters*. Am. Inst. Phys., New York, p. 17
- Schawinski K., 2012, *proc. Frank N. Bash Symp., New Horizons in Astronomy*, preprint ([arXiv:1206.2661](https://arxiv.org/abs/1206.2661))
- Schawinski K. et al., 2007a, *ApJS*, 173, 512
- Schawinski K., Thomas D., Sarzi M., Maraston C., Kaviraj S., Joo S.-J., Yi S. K., Silk J., 2007b, *MNRAS*, 382, 1415
- Schawinski K. et al., 2009a, *MNRAS*, 396, 818
- Schawinski K. et al., 2009b, *ApJ*, 690, 1672
- Schawinski K., Virani S., Simmons B., Urry C. M., Treister E., Kaviraj S., Kushkuley B., 2009c, *ApJ*, 692, L19
- Schawinski K. et al., 2010a, *ApJ*, 711, 284
- Schawinski K., Dowlin N., Thomas D., Urry C. M., Edmondson E., 2010b, *ApJ*, 714, L108
- Schawinski K., Treister E., Urry C. M., Cardamone C. N., Simmons B., Yi S. K., 2011, *ApJ*, 727, L31
- Schawinski K., Simmons B. D., Urry C. M., Treister E., Glikman E., 2012, *MNRAS*, 425, L61
- Schiminovich D. et al., 2007, *ApJS*, 173, 315
- Schmidt M., 1959, *ApJ*, 129, 243
- Shapiro K. L. et al., 2010, *MNRAS*, 402, 2140
- Sheth K. et al., 2008, *ApJ*, 675, 1141

- Silverman J. D. et al., 2008, *ApJ*, 675, 1025
 Simmons B. D., Urry C. M., Schawinski K., Cardamone C., Glikman E., 2012, *ApJ*, 761, 75
 Skibba R. A. et al., 2009, *MNRAS*, 399, 966
 Skibba R. A. et al., 2012, *MNRAS*, 423, 1485
 Skrutskie M. F. et al., 2006, *AJ*, 131, 1163
 Sodré L., Ribeiro da Silva A., Santos W. A., 2013, *MNRAS*, 434, 2503
 Springel V., Di Matteo T., Hernquist L., 2005, *ApJ*, 620, L79
 Strateva I. et al., 2001, *AJ*, 122, 1861
 Taylor M. B., 2005, in Shopbell P., Britton M., Ebert R., eds, *ASP Conf. Ser. Vol. 347, Astronomical Data Analysis Software and Systems XIV*. Astron. Soc. Pac., San Francisco, p. 29
 Taylor M., 2011, *Astrophysics Source Code Libr.*, 1010
 Teng S. H. et al., 2012, *ApJ*, 753, 165
 Tinsley B. M., 1968, *ApJ*, 151, 547
 Tinsley B. M., Gunn J. E., 1976, *ApJ*, 203, 52
 Tinsley B. M., Larson R. B., 1978, *ApJ*, 221, 554
 Tonnesen S., 2011, in Salviander S., Green J., Pawlik A., eds, *Proc. Frank N. Bash Symp., New Horizons in Astronomy*. Available at: <http://pos.sissa.it/cgi-bin/reader/conf.cgi?confid=149>
 Treister E., Schawinski K., Urry C. M., Simmons B. D., 2012, *ApJ*, 758, L39
 van den Bergh S., 1976, *ApJ*, 206, 883
 Vollmer B., 2013, in Oswalt T. D., Keel W. C., eds, *The Influence of Environment on Galaxy Evolution*. Springer, Netherlands, p. 207
 Wetzel A. R., Tinker J. L., Conroy C., van den Bosch F. C., 2013, *MNRAS*, 432, 336
 Wild V., Kauffmann G., Heckman T., Charlot S., Lemson G., Brinchmann J., Reichard T., Pasquali A., 2007, *MNRAS*, 381, 543
 Williams R. J., Quadri R. F., Franx M., van Dokkum P., Labbé I., 2009, *ApJ*, 691, 1879
 Wolf C. et al., 2009, *MNRAS*, 393, 1302
 Wong O. I. et al., 2012, *MNRAS*, 420, 1684
 Wyder T. K. et al., 2007, *ApJS*, 173, 293
 Yang X., Mo H. J., van den Bosch F. C., Pasquali A., Li C., Barden M., 2007, *ApJ*, 671, 153
 Yi S. K. et al., 2005, *ApJ*, 619, L111
 York D. G. et al., 2000, *AJ*, 120, 1579

APPENDIX A: DOES THE EARLY STAR FORMATION HISTORY OF MAIN SEQUENCE GALAXIES HAS AN APPRECIABLE EFFECT ON POST-QUENCHING EVOLUTION?

We use the $NUVur$ diagram (Fig. 7) to constrain the quenching time-scales of galaxies using a simple model star formation history: constant SFR for 9 Gyr, followed by an exponential decline

of varying time-scale τ . The model assumes that all star-forming galaxies are on the main sequence prior to the quenching event, as is appropriate to our goal of describing the bulk of normal galaxies. But do all galaxies on the main sequence have comparable colours; that is, are the starting points of all star-forming galaxies comparable? In order to test this, we plot the colour evolution of $u - r$ and $NUV - u$ in Fig. A1. We explore a range of models:

(i) Model 1 (black line): fiducial model of constant SFR, followed by exponential decay, in this case with $\tau_{\text{quench}} = 100$ Myr.

(ii) Model 2 (green dashed line): same as Model 1, but with Gaussian random perturbations in the amplitude prior to quenching with a dispersion of a factor 2.

(iii) Model 3 (light blue line): rather than a constant SFR, the pre-quenching star formation history is a gently exponentially declining SFR ($\tau = 5.0$ Gyr), which builds up a more significant old stellar population by the time of quenching. The model is tuned to have an SSFR at the quenching time $t_{\text{quench}} = 9$ Gyr that is at the lower edge of the Main Sequence.

(iv) Model 4 (red line): same as Model 3, but with a more strongly exponentially declining SFR prior to quenching ($\tau = 2.5$ Gyr). This Model has an SSFR 1 dex below the Main Sequence at t_{quench} , and thus is (just a bit) outside the suite of galaxies whose quenching is discussed in this paper.

These model tracks demonstrate that a wide range of initial star-formation histories create galaxies with similar main sequence $u - r$ and $NUV - u$ colours at the point of quenching. This is because $NUV - u$ and $u - r$ colours are dominated by current and recent stellar populations. Thus, star formation histories that place a galaxy on the main sequence will also result in similarly blue colours. Once quenching sets in, the movement towards the red is similarly governed by young stellar populations and thus the time-scales are similar regardless of the pre-quenching star formation history.

We combine these diagrams and place the same four model tracks on a version of Fig. 7 in Fig. A2. We show how those four model tracks evolve: Models 1, 2 and 3 are virtually on top of each other and indicate a short quenching time-scale, as expected from the assumed $\tau_{\text{quench}} = 100$ Myr. Model 4 (red) – which is ruled out due to its low SSFR – is offset and would indicate somewhat longer time-scales, but is still not comparable to the ‘slow’ quenching tracks which best fit late-type galaxies. We conclude that the time-scales deduced from the $NUVur$ diagram are robust with respect to initial star formation histories because the main sequence dictates similar colours at the point of quenching.

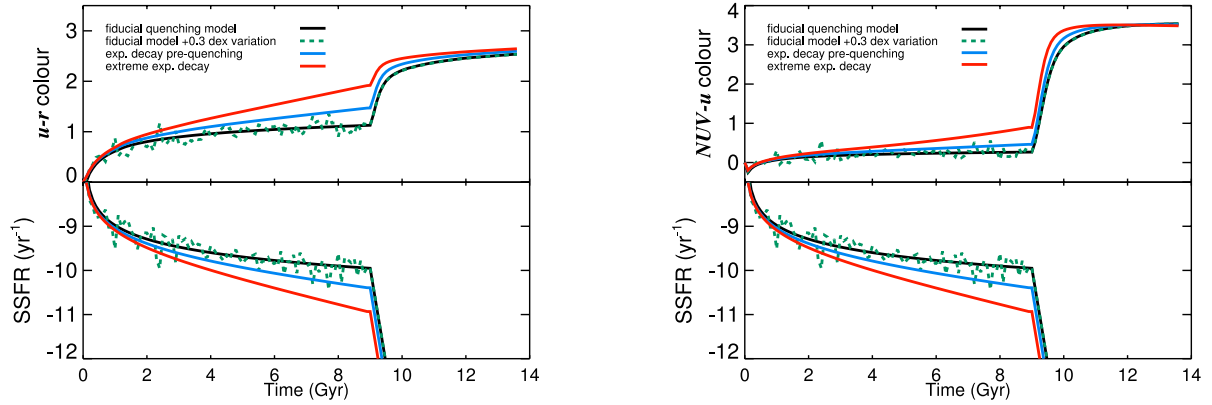


Figure A1. Evolution of $u - r$ colour (left) and $NUV - u$ colour (right) as a function of time for a set of four models. Below the colour evolution of each model, we show the $sSFR$ as a function of time. Model 1 (black line): fiducial model of constant SFR, followed by exponential decay, in this case with $\tau_{\text{quench}} = 100$ Myr. Model 2 (green dashed line): same as Model 1, but with random perturbations prior to quenching. Model 3 (light blue line): rather than a constant SFR, the pre-quenching star formation history is a gently exponentially declining SFR. This SFR builds up a more significant old stellar population by the time of quenching. The model is tuned to have an $sSFR$ at the quenching time $t_{\text{quench}} = 9$ Gyr that is at the lower edge of the Main Sequence. Model 4 (red line): same as Model 3, but with a more strongly exponentially declining SFR prior to quenching. This Model has an $sSFR \sim 1$ dex below the Main Sequence at t_{quench} . Due to its low $sSFR$ at t_{quench} , Model 4 is incompatible with the Main Sequence. The other models, do not show significant offsets from the fiducial quenching model as they all have the following salient features: at t_{quench} , they have blue cloud $u - r$ and $NUV - u$ colours, and after the quenching event, they become redder at essentially the same rate. Thus, all SFHs which place a galaxy on the main sequence at the point of quenching yield similar quenching time-scale.

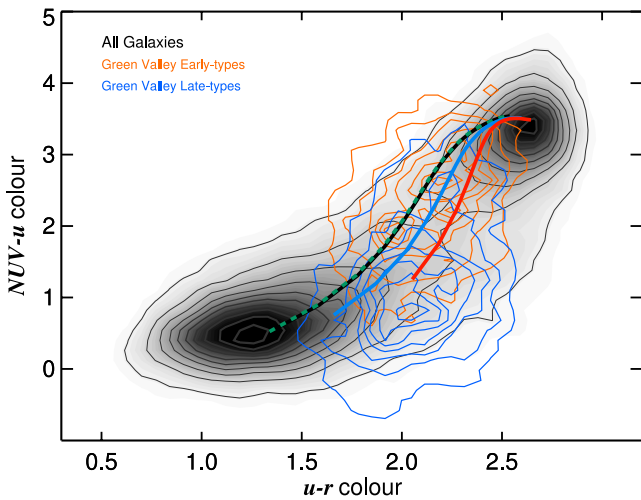


Figure A2. The $NUVur$ colour diagram, similar to Fig. 7, with the same Model tracks shown as on Fig. A1. All models that are on the main sequence at the time of quenching (black, green, light blue) yield a short quenching. The red model, which is incompatible with the Main Sequence due to having a low $sSFR$ at the quenching time, is somewhat offset, but still yields a short quenching time-scale on the $NUVur$ diagram. Together with Fig. A1, this Figure illustrates the robustness of the $NUVur$ diagram as a quenching time and that all reasonable star formation histories that end up on the main sequence are blue, and reasonable starting points for our quenching model.

This paper has been typeset from a $\text{\TeX}/\text{\LaTeX}$ file prepared by the author.